

Kinetic energy and the Born-Green-Yvon method for fermion quantum fluids

C. E. Campbell and K. E. Kürten*

School of Physics and Astronomy, University of Minnesota, Minneapolis, Minnesota 55455

E. Krotscheck

Department of Physics, State University of New York, Stony Brook, New York 11794

(Received 17 August 1981)

The Born-Green-Yvon (BGY) equations for two-body distribution functions of fermion-Jastrow many-body trial functions are derived using a diagrammatic method. Also derived are the Jackson-Feenberg and Pandharipande-Bethe expressions for the kinetic energy of this function in terms of partial two- and three-body distribution functions. Simple approximations for these three-body functions are then used in the BGY equations and the kinetic energies are solved for the ground state of liquid ^3He .

I. INTRODUCTION

There has been much progress in recent years in the microscopic theory of fermion quantum fluids, the most studied of which are liquid ^3He , neutron matter, and nuclear matter.¹⁻⁷ The most successful approach has been the Feenberg-Jastrow variational method (and its generalizations) combined with the method of correlated basis functions. Of the numerous procedures for calculating the necessary matrix elements in this method, the fermion generalization of the hypernetted chain method (FHNC) has gained widest acceptance.^{8,9} We recently pointed out, however, that one can gain some new insights into this general problem by developing the fermion generalization of the Born-Green-Yvon method (FBGY) as an alternative to the FHNC method.^{10,11} Perhaps the most illuminating insight is that the FBGY method is intimately related to several often-used expressions for the kinetic-energy expectation value in a fermion-Jastrow function,⁴ and provides the "natural" way to find approximations which preserve the identity of these alternative expressions.

In this paper we employ a diagrammatic method to derive the FBGY equations. At the same time we give a complete derivation of analytic expressions for the three most common expressions for the kinetic energy—Jackson-Feenberg (JF), Clark-Westhaus (CW), and Pandharipande-Bethe (PB)—and discuss a fourth expression which we find convenient. We then explore approximation schemes which are sympathetic to the structure of the

FBGY equations, and apply the method to the problem of the normal ground state of liquid ^3He . We find that the numerical accuracy of the simplest approximation scheme is better than the FHNC/0 approximation while no more difficult to implement.

The remainder of this section contains a review of elements of the Jastrow method which we consider important for our present discussion, including certain elements of the diagrammatic procedure which led to the FHNC method. Sections II–V detail the formal theory of both kinetic energy and the FBGY equations. Our approximations are defined in Sec. VI and applied to liquid ^3He in Sec. VII. In Sec. VIII we discuss the results of the present work and other integral equation methods applied to the fermion-Jastrow theory of liquid ^3He .

The Feenberg-Jastrow variational approach and the method of correlated basis functions was devised in part to deal quantitatively with the strong short-range interactions present in the above-mentioned quantum fluids.¹⁻⁴ The general approach is to consider wave functions for the N -body system of the form

$$\psi(1, \dots, N) = \psi_c(1, \dots, N) \Phi_m(1, \dots, N), \quad (1.1)$$

where ψ_c is a symmetric correlation function (or operator⁷) which is chosen to deal with the short-range correlations in an efficient way, and Φ_m are model functions incorporating other properties of the system, e.g., the correct statistics. The simplest choices are due to Jastrow¹²

$$\psi_c(1, \dots, N) = \psi_J(\vec{r}_1, \dots, \vec{r}_N) \equiv \prod_{i < j}^N f(r_{ij}) , \quad (1.2)$$

which can be made to vanish upon close approach of two particles by an appropriate choice of f . The ground state of a boson liquid such as liquid ^4He may be approximated by the choice $\Phi_m = 1$, while for a fermion liquid such as ^3He or neutron matter a useful trial ground state is obtained by the choice Φ_m equal to the ground state of the noninteracting system, i.e., a Slater determinant with all of the single-particle states inside the Fermi sea.

$$g_n(\vec{r}_1 \cdots \vec{r}_n) = \frac{(N-n)!}{\rho^n N! I_0} \sum_{\sigma_1 \cdots \sigma_n} \int d\tau_{n+1} \cdots d\tau_N |\psi(1 \cdots N)|^2 , \quad (1.3)$$

where I_0 is the normalization integral, ρ is the number N over volume, σ_i refers to spin (isospin) when appropriate, and the integral over τ_i includes the sum over these discrete degrees of freedom. The average of a two-body potential energy $\langle V \rangle$ and the x-ray structure factor $S(k)$ require only the radial distribution function $g(r)$ defined by

$$g(r_{12}) = g_2(\vec{r}_1, \vec{r}_2) ,$$

with the result

$$\langle V \rangle = \frac{N\rho}{2} \int g(r) V(r) d^3r \quad (1.4)$$

and

$$S(k) = 1 + \rho \int e^{i\vec{k}\cdot\vec{r}} [g(r) - 1] d^3r . \quad (1.5)$$

With the choice of ψ_c in the Jastrow form [Eq. (1.2)], the kinetic-energy expectation value requires only $g(r_{12})$ and $g_3(\vec{r}_1, \vec{r}_2, \vec{r}_3)$. A three-body potential would require g_3 while the second-order light-scattering intensity requires a linear combination of g , g_3 , and g_4 .

For the fermion liquids of interest near their saturation density and above, the task of calculating these quantities with the simplest trial function—the Jastrow function multiplying a Slater determinant—is more difficult than the corresponding boson problem. While low-density systems may be treated by a low-order Ursell-Mayer type of cluster expansion of the Jastrow factor, liquid ^3He and nuclear matter require a better account of the short-range correlations. Wu and Feenberg took an important step toward that goal by performing the cluster expansion on the Slater determinant squared (a statistical cluster expansion)

The function f in the Jastrow correlation factor in each of these cases is chosen variationally (parameter variation,^{13–18} Euler-Lagrange functional variation,^{19–25} or a combination of the two^{26,7}) by minimizing the expectation value of the Hamiltonian in these trial ground states. While elaborations of this approach have proven useful,^{3,20,27–30} all begin at this point and are faced with the general problem of calculating matrix elements in these correlated states of the form of Eq. (1.2).

Many of the properties of a quantum fluid may be expressed in terms of low-index distribution functions for the square of the trial function, defined by

while keeping the bosonlike correlation factor intact.¹ The results of such a calculation are expressed in terms of low-index distribution functions for the correlation function ψ_c alone. These distribution functions are calculated by the simpler boson procedures (discussed further below).^{15,17}

While generalizations of the Wu-Feenberg approach have apparently produced relatively good results for the energy as a function of density,^{31,32} the most commonly used procedure for dealing with the fermion-Jastrow wave function is the fermion hypernetted chain method (FHNC).^{8,9,4} This is a generalization of the hypernetted chain method (HNC) derived originally for classical fluids³³ and applied subsequently to the boson-Jastrow ground-state problem in liquid ^4He .^{19,16,17,34,35} It is a formal chain-parallel resummation of the Ursell-Mayer cluster expansion for the radial distribution function $g(r_{12})$ which produces a nonlinear integral equation for $g(r_{12})$ in terms of the Jastrow pseudopotential $u(r_{12})$ [or the dimensionless potential $-V(r_{12})/k_B T$ for a classical fluid at temperature T], defined by

$$f(r_{12}) = \exp\left[\frac{1}{2}u(r_{12})\right] . \quad (1.6)$$

The exact result is written concisely as

$$g(r) = \exp[u(r) + N(r) + E(r)] , \quad (1.7)$$

where $N(r)$ is the sum of all nodal diagrams and the bridge function $E(r)$ is the sum of all elementary diagrams, both of which are illustrated schematically in Fig. 1. The renormalized bonds in the cluster expansion are

$$\Gamma(r) = g(r) - 1 , \quad (1.8)$$

FIG. 1. Schematic diagrammatic expressions for the nodal sum $N(r)$ and bridge function $E(r)$ for a boson-Jastrow function, expressed in terms of the renormalized bond $\Gamma(r)$.

which is the Fourier transform of $S(k) - 1$ [Eq. (1.5)]. Thus, the nodal sum can be written in the closed form

$$N(r) = \frac{1}{(2\pi)^3 \rho} \int e^{-i\vec{k}\cdot\vec{r}} \frac{[S(k) - 1]^2}{S(k)} d^3k \quad (1.9)$$

The elementary diagrams are non-nodal (cannot be broken into two parts at a single point) and non-compound (cannot be factorized). The simplest such diagram $E_4(r)$ involves two internal and two external points; it is the first term in $E(r)$ in Fig. 1. The second term is the simplest five-point diagram. (There are four more topologically distinct five-point elementary diagrams.) The approximation commonly called the HNC approximation but more properly called the HNC/0 approximation is obtained by setting $E(r)$ to zero in Eq. (1.7) and solving the resulting nonlinear integral equation for $g(r)$ from a given $u(r)$. The HNC/4 approximation, obtained by including only $E_4(r)$, and estimates of contributions of E_5 and higher have been done for ${}^4\text{He}$ and give evidence of rapid convergence in both $g(r)$ and the energy per particle.³⁶

The fermion generalization of the HNC method was complicated by the presence of the Slater determinant in the wave function. However, since it is the square of the wave function which enters into the definition of the distribution functions g_n , Eq. (1.2), the fact that the square of the determinant is the determinant of the square can be used to isolate the statistical information in a single determinant of two-body functions³⁷

$$|\psi(1, \dots, N)|^2 = \left[\prod_{i < j} \exp[u(r_{ij})] \right] \times \det[\beta(\vec{r}_i, \sigma_i, \vec{r}_j, \sigma_j)], \quad (1.10)$$

where $\beta(x_i, x_j)$ is the one-body density matrix of the uncorrelated system ($\psi_c = 1$) which in the case

of a uniform system has the form

$$\beta(x_i, x_j) = l(k_f r_{ij}) \delta_{\sigma_i, \sigma_j} / \nu, \quad (1.11)$$

where ν is the single-particle level degeneracy due to the discrete degrees of freedom ($\nu = 2$ for ${}^3\text{He}$, $\nu = 4$ for nuclear matter), k_f is the Fermi wave number, and $l(z)$ is the Slater function

$$l(z) = 3(\sin z - z \cos z) / z^3. \quad (1.12)$$

Because of this determinant factor, the Ursell-Mayer expansion must be supplemented by directed exchange bonds $\beta(x_i, x_j)$ which are chained to form permutation polygons.

Fantoni and Rosati,⁸ and Krotscheck and Ristig⁹ showed how to incorporate these statistical bonds into the HNC resummation to produce the FHNC method.⁴ The result, some parts of which we will discuss further below, is a coupled set of equations similar to the boson HNC equation [Eq. (1.7)], complete with a set of elementary diagrams which can be set to zero to produce the FHNC/0 approximation or, retaining four-point elementary diagrams, to produce the FHNC/4 approximation, etc. Application of these approximations to neutron matter and liquid ${}^3\text{He}$ (Ref. 38) show reasonable convergence to the energy and radial distribution function as obtained by Monte Carlo evaluation with the same Jastrow function,³⁹ although the results for liquid ${}^3\text{He}$ show a significant discrepancy in the energy as the density is increased from equilibrium. Another approximation scheme, FHNC/C gives similar results for the energy and correct long-wavelength behavior of $S(k)$.⁴⁰ This approximation has significant advantages in that it can be solved for liquid ${}^3\text{He}$ under elevated pressure^{25,41} and the solutions of the optimization problem are consistent with exact long-wavelength properties.⁴²

The HNC method is only one of several methods which have been successful in the calculations of properties of classical fluids and boson quantum fluids. A similar cluster resummation scheme is the Percus-Yevick approximation.^{16,19} Both are predated, however, by the Born-Green-Yvon (BGY) method.⁴³ These alternative methods have given different insights into the general structure of the theory and, in some instances, improved results. A good example is the convergence of the HNC/ n and BGY/ n calculations of $g(r)$ and E to common results, illustrated for liquid ${}^4\text{He}$ in Ref. 36.

The BGY method is based upon the BGY hierarchy of equations for the distribution func-

tions obtained by operating with $\vec{\nabla}_1$ on the definition of g_n , Eq. (1.3). For the uniform fluid the $n=1$ equation is trivial. The $n=2$ equation is an equation for the radial distribution function which, in the case of a boson-Jastrow wave function [Eq. (1.7)], involves only $u(r_{12})$ and $g_3(\vec{r}_1, \vec{r}_2, \vec{r}_3)$:

$$\vec{\nabla}_1 g(r_{12}) = g(r_{12}) \vec{\nabla}_1 u(r_{12}) + \rho \int g_3(\vec{r}_1, \vec{r}_2, \vec{r}_3) \vec{\nabla}_1 u(r_{13}) d^3 r_3. \quad (1.13)$$

Since ψ involves only the two-body function $u(r)$, g_3 can be expressed as a functional of g .⁴⁴ Consequently Eq. (1.13) is an integral equation for $g(r)$. It is made tractable by approximating the dependence of g_3 or g .^{44,36} The simplest choice is the Kirkwood superposition approximation (KSA), where g_3 is approximated by

$$g_3(\vec{r}_1, \vec{r}_2, \vec{r}_3) = g(r_{12})g(r_{23})g(r_{31}). \quad (1.14)$$

The resulting approximate integral-differential equation, written in the form,

$$\vec{\nabla}_1 \ln g(r_{12}) = \nabla_1 u(r_{12}) + \rho \int g(r_{13})g(r_{23}) \nabla_1 u(r_{13}) d^3 r_3 \quad (1.15)$$

is the BGY approximation for $g(r)$.

In the fermion case, the presence of the factor $\det \beta_{ij}$ in ψ^2 produces two additional terms on the right-hand side of Eq. (1.14), one proportional to $\vec{\nabla}_1 l(k_f r_{12})$ and one in the integral proportional to $\vec{\nabla}_1 l(k_f r_{13})$:

$$\begin{aligned} \vec{\nabla}_1 g(r_{12}) = & g(r_{12}) \vec{\nabla}_1 u(r_{12}) + \gamma(r_{12}) \nabla_1 l(k_f r_{12}) / v \\ & + \rho \int [g_3(\vec{r}_1 \vec{r}_2 \vec{r}_3) \vec{\nabla}_1 u(r_{13}) \\ & + \gamma_3(\vec{r}_1 \vec{r}_2 \vec{r}_3) \vec{\nabla}_1 l(k_f r_{13}) / v]. \end{aligned} \quad (1.16)$$

Since the determinant is not a simple exponential, the new functions $\gamma(r_{12})$ and $\gamma_3(\vec{r}_1 \vec{r}_2 \vec{r}_3)$ are not simple distribution functions. These new functions require additional definitions and additional equations as is the case in the FHNC method. In our earlier work on the FBGY method,^{10,11} we attempted to define these new functions and the fermion generalization of the superposition approximation without reference to the diagrammatic analysis, as was done originally for the classical fluids. This approach, however, produced somewhat incomplete results due to the difficulty of defining certain sets of "non-nodal" diagrams entirely in terms of distribution functions. We will comment more on this difficulty in some more detail below.

In this paper we make use of a diagrammatic analysis to derive the set of $n=2$ BGY equations. We begin in Sec. II with the definition of partial two-body and three-body distribution functions classified according to the exchange characteristics of their external points. These are then decomposed further to exhibit their nodal structure. This analysis is then used in Sec. III to derive complete expressions for the three commonly used forms of the fermion-Jastrow kinetic energy (Jackson-Feenberg, Clark-Westhaus, and Pandharipande-Bethe).⁴ Section IV contains the derivation of the $n=2$ FBGY equations. We also show how one uses these equations to derive the alternative expressions for the kinetic energy beginning with one of them. In the process we gain some insight into the relationship between the FBGY approach and the FHNC approach. The fermion generalization of the Kirkwood superposition approximation is presented in Sec. VI. There, it is seen that the natural approximation scheme preserves the equivalence of the different expressions for the kinetic energy (in contrast to the natural approximations within the FHNC method). Numerical results for liquid ³He are compared to other results in Sec. VII. We close with a summary and discussion in Sec. VIII.

II. PARTIAL DISTRIBUTION FUNCTIONS AND NODAL EQUATIONS

Some general features of the functional structure of the reduced distribution functions $g_n(\vec{r}_1 \cdots \vec{r}_n)$ come naturally out of the fermion generalization of an Ursell-Mayer diagrammatic analysis which leads to the FHNC method. As we noted in the last section the diagrammatic elements are both the dynamical bonds $h(r_{ij}) = \exp[u(r_{ij})] - 1$ (present in a Jastrow-boson or classical theory) and the exchange bonds $l(k_f r_{ij})$. The diagram rules for the dynamical correlation lines are identical to the boson (or classical) case while the rules for the exchange bonds follow from the fact that $\det l(k_f r_{mn})$ can be written as the sum of the product of all exchange polygons, with every coordinate \vec{r}_p having exactly one exchange bond entering, $l(k_f \vec{r}_{mp})$ and one (possibly the same) exchange bond leaving, $l(k_f \vec{r}_{pn})$. These are represented in Figs. 2(a) and 2(b), where $l(k_f r_{ij})$ is a line with an arrow from point i to point j . Finally, before classifying various diagrammatic contributions one must make use of the convolution property of the statistical bonds

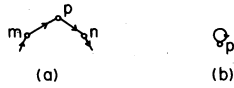


FIG. 2. (a) Exchange bonds in an exchange polygon. (b) Exchange bond of coordinate p with itself.

$$\frac{\rho}{v} \int l(k_f r_{13}) l(k_f r_{32}) d^3 r_3 = l(k_f r_{12}), \quad (2.1)$$

which is a consequence of the Pauli exclusion principle. In diagrammatic terms, this means that no diagram appears which contains an integral point (integration point) which is only exchange-correlated with other particles. The importance of this result is clear from the example of the free Fermi gas, where there are no dynamical bonds and thus no internal points after the application of (2.1). Then the free-particle radial distribution g_F becomes

$$g_F(r_{12}) = l(k_f r_{11}) l(k_f r_{22}) - l(k_f r_{12}) l(k_f r_{21}) / v = 1 - l(k_f r_{12}) l(k_f r_{21}) / v. \quad (2.2)$$

In the more general case, $g(r_{12}) - 1$ can be shown to be the sum of all irreducible diagrams containing the two external points (1 and 2) which are constructed from dynamical and exchange bonds, and in which all internal points are at least singly connected to the remainder of the diagram. It is then convenient to regroup these diagrams in accord with the exchange character of their external points:

$$g(r_{12}) - 1 = \Gamma_{dd}(r_{12}) + \Gamma_{de}(r_{12}) + \Gamma_{ed}(r_{12}) + \Gamma_{ee}(r_{12}), \quad (2.3)$$

where an external point labeled d is a direct point (no exchange bond with any other point) and one labeled e is connected by an exchange bond to some other point.

The function $\Gamma_{ee}(r_{12})$ includes among others all of the terms in $g(r_{12})$ proportional to $l(k_f \vec{r}_{12})$ or $l(k_f \vec{r}_{21})$ and thus is decomposed as

$$\Gamma_{ee}(r_{12}) = \hat{g}_{ee}(r_{12}) + v^{-1} \times [l(k_f \vec{r}_{12}) l(k_f \vec{r}_{21}) g_{dd}(r_{12}) - l(k_f \vec{r}_{12}) \Gamma_{cc}(\vec{r}_{21}) - l(k_f \vec{r}_{21}) \Gamma_{cc}(\vec{r}_{12})], \quad (2.4)$$

where \hat{g}_{ee} is defined as Γ_{ee} except that it contains no exchange bonds which are direct links between the external points, the function g_{dd} is a dressed version of $f^2(r_{12})$;

$$g_{dd}(r_{12}) = \Gamma_{dd}(r_{12}) + 1, \quad (2.5)$$

and $\Gamma_{cc}(\vec{r}_{12})$ is a dressed exchange line between points 1 and 2:

$$\Gamma_{cc}(\vec{r}_{12}) = l(k_f r_{12}) + \Gamma_{dd}(r_{12}) l(k_f r_{12}) + \hat{g}_{cc}(r_{12}). \quad (2.6)$$

The first two terms in (2.6) exhibit all terms in $\Gamma_{cc}(r_{12})$ proportional to $l(k_f \vec{r}_{12})$ so that $\hat{g}_{cc}(\vec{r}_{12})$ is that part of $\Gamma_{cc}(\vec{r}_{12})$ which has at least one internal point on the exchange line linking 1 and 2. With these definitions, Eq. (2.3) can be rewritten so as to explicitly exhibit all exchange lines between the external points:

$$g(r_{12}) = [1 - l(k_f r_{12}) l(k_f r_{21}) / v] g_{dd}(r_{12}) + \Gamma_{de}(r_{12}) + \Gamma_{ed}(r_{12}) - v^{-1} [l(k_f r_{12}) \hat{g}_{cc}(\vec{r}_{21}) + l(k_f r_{21}) \hat{g}_{cc}(\vec{r}_{12})] + \hat{g}_{ee}(r_{12}). \quad (2.7)$$

This equation for $g(r_{12})$ is represented graphically in Fig. 3(a), with each of the partial two-body distribution functions represented as a "two-sided" polygon [the lens-shaped figures in Figs. 3(b)–3(f)] to be thought of as a black box containing all of the connected internal points. The $\Gamma_{\alpha\beta}(r_{12})$, which are best thought of as dressed bonds with external points of an α and β character, respectively, are defined graphically in Fig. 3(c) and Fig. 4. Note that by comparing Eq. (2.2) to Eq. (2.7) it can be seen that $g_{dd} = 1$ while Γ_{de} , \hat{g}_{cc} , and \hat{g}_{ee} all vanish in the free Fermi gas.

The three-body distribution function $g_3(\vec{r}_1, \vec{r}_2, \vec{r}_3)$ can also be decomposed into partial distribution functions according to the exchange character of

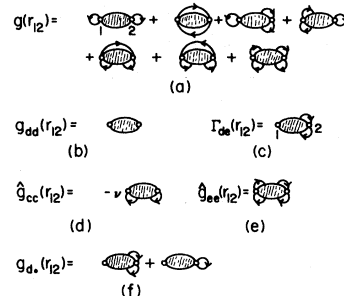


FIG. 3. Schematic diagrammatic expression for $g(r_{12})$ in terms of partial distribution functions (b)–(f) exhibiting the termination points of the statistical correlation lines which are attached to the external points 1 and 2.

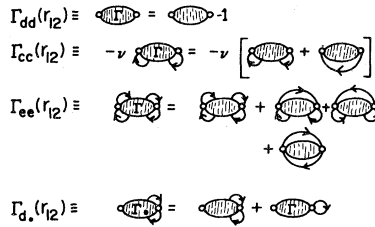


FIG. 4. Together with Fig. 3(c), the dressed bonds between two points 1 and 2.

the three external points. While there are 34 terms in this expression compared to the seven terms in Eq. (2.7) for $g(r_{12})$, it is composed of only six different partial distribution functions: g_{ddd} , g_{dde} , \hat{g}_{ccd} , \hat{g}_{eee} , \hat{g}_{eed} , and \hat{g}_{cce} . These are represented graphically by the shaded triangles in Fig. 5. Completing these diagrams with external exchange bonds in all possible ways and taking all distinct permutations of the external points gives all of the terms included in g_3 .

Ornstein and Zernike first introduced the concept of a direct correlation function to facilitate the treatment of long-range correlations in classical fluids,⁴⁵ and it plays a similar role in the theory of quantum fluids. Graphically a direct correlation function $X(r_{12})$ is the sum of non-nodal diagrams which appear in the two-body correlation function $g(r_{12}) - 1$. For the classical or boson system, the relationship between $g - 1$ and X is

$$g(r_{12}) - 1 = X(r_{12}) + \rho \int [g(r_{13}) - 1] X(r_{32}) d^3 r_3 . \tag{2.8}$$

The second term is the sum of the nodal diagrams $N(r_{12})$ which can also be written as in Eq. (1.9).

In fermion quantum fluids the Pauli exclusion principle introduces long-range correlations which are conveniently dealt with through the generalization of this type of nodal equation. The non-nodal sums (direct correlation functions) are subscripted

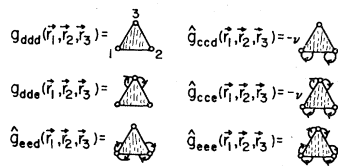


FIG. 5. Partial three-body distribution functions which appear in the diagrammatic expression for the full three-body distribution function $g_3(\vec{r}_1, \vec{r}_2, \vec{r}_3)$.

according to the exchange character, and the nodal terms are compounded with attention paid to the restriction that each point can be part of only one exchange cycle:

$$\Gamma_{dd}(r_{12}) = X_{dd}(r_{12}) + \rho \int [X_{de}(r_{13}) \Gamma_{dd}(r_{32}) + X_{dd}(r_{13}) \Gamma_{dd}(r_{32}) + X_{dd}(r_{13}) \Gamma_{ed}(r_{32})] d^3 r_3 , \tag{2.9}$$

$$\Gamma_{de}(r_{12}) = X_{de}(r_{12}) + \rho \int [X_{de}(r_{13}) \Gamma_{de}(r_{32}) + X_{dd}(r_{13}) \Gamma_{de}(r_{32}) + X_{dd}(r_{13}) \Gamma_{ee}(r_{32})] d^3 r_3 , \tag{2.10}$$

$$\Gamma_{ee}(r_{12}) = X_{ee}(r_{12}) + \rho \int \{ [X_{ee}(r_{13}) + X_{ed}(r_{13})] \Gamma_{de}(r_{32}) + X_{ed}(r_{13}) \Gamma_{ee}(r_{32}) \} d^3 r_3 , \tag{2.11}$$

and

$$\Gamma_{cc}(r_{12}) = l(k_f r_{12}) - \nu X_{cc}(r_{12}) + \rho \int X_{cc}(r_{13}) \Gamma_{cc}(r_{32}) d^3 r_3 . \tag{2.12}$$

These equations can be taken as definitions of the $X_{\alpha\beta}$ except that Eq. (2.12) defines X_{cc} only for wave numbers larger than the Fermi wave number k_F . In that case the graphical definition must supplement (2.12). The second term on the right-hand side of each of these equations is the corresponding nodal function, $N_{\alpha\beta}$.

The convolution property of Eq. (2.1) together with the cc nodal equation (2.12) can be combined to demonstrate an important convolution property of the dressed exchange bond:

$$\frac{\rho}{\nu} \int [\Gamma_{cc}(r_{13}) - l(k_F r_{13})] l(k_F r_{32}) d^3 r_3 = 0 , \tag{2.13}$$

provided that $\tilde{X}_{cc}(k) \neq 1$ for $k < k_F$. Thus, any diagram which has an internal point with only l entering and only $[\Gamma_{cc} - l]$ leaving or vice versa, integrates to zero. This is a special realization of a more general cancellation property of exchange diagrams introduced by the Pauli principle.^{9,42}

In the next sections we derive the FBGY equations and expressions for the kinetic energy, all of which involve (partial) three-body distribution functions with integration over one or three of the external points. It will be seen that in some cases these external points become effectively internal points, and cannot, therefore, be correlated only by exchange bonds or only by one exchange and one

cc bond. Consequently, it is convenient to examine the nodal properties of the partial three-body functions \hat{g}_{ccd} and $\hat{g}_{cc\cdot}$. We first define auxiliary functions Γ_{ccd} and $\Gamma_{cc\cdot}$ similarly to the definition of Γ_{cc} :

$$\Gamma_{cc\cdot}(\vec{r}_1, \vec{r}_2, \vec{r}_3) = \hat{g}_{c\cdot c}(\vec{r}_1, \vec{r}_2, \vec{r}_3) + l(k_f r_{12})g_{dde}(\vec{r}_1, \vec{r}_2, \vec{r}_3) + \Gamma_{ccd}(\vec{r}_1, \vec{r}_2, \vec{r}_3) - \nu^{-1} [l(k_f r_{13})l(k_f r_{23})g_{ddd}(\vec{r}_1, \vec{r}_2, \vec{r}_3) + l(k_f r_{13})\hat{g}_{d\cdot c}(\vec{r}_1, \vec{r}_2, \vec{r}_3) + l(k_f r_{23})\hat{g}_{dc\cdot}(\vec{r}_1, \vec{r}_2, \vec{r}_3)], \quad (2.15)$$

which are shown graphically in Fig. 6. Since there are three external points in these functions, there are diagrammatic parts of each function which are nodal in one point, in two points, or in all three points, where being nodal in point p means there is an internal point through which pass all diagrammatic paths connecting point p to any other external point. Three-body functions $Z_{\alpha\beta\gamma}$, $Y_{\alpha\beta\gamma}$, and $X_{\alpha\beta\gamma}$ are defined as functions which are non-nodal in one, two, or three external points. In particular, we need Z_{ccd} , Y_{ccd} , and $Z_{cc\cdot}$, defined in the following equations and in Fig. 7:

$$\Gamma_{cc\cdot}(\vec{r}_1, \vec{r}_2, \vec{r}_3) = g_{d\cdot}(r_{13})\Gamma_{cc}(r_{12}) - \Gamma_{cc}(r_{13})\Gamma_{cc}(r_{32})/\nu + Z_{c\cdot c}(\vec{r}_1, \vec{r}_3; \vec{r}_2) - \frac{\rho}{\nu} \int Z_{c\cdot c}(\vec{r}_1, \vec{r}_3; \vec{r}_4)\Gamma_{cc}(r_{42})d^3r_4, \quad (2.18)$$

where $Z_{c\cdot c}(1,3;2)$ is non-nodal in point 2 and

$$g_{d\cdot}(r_{12}) \equiv \Gamma_{de}(r_{12}) + g_{dd}(r_{12}). \quad (2.19)$$

Note that the convolution property of Γ_{cc} [Eq. (2.13)] and these definitions of Z and Y combine to give similar convolution properties for three-body functions:

$$\frac{\rho}{\nu} \int \Gamma_{ccd}(\vec{r}_1, \vec{r}_4, \vec{r}_3)l(k_F r_{42})d^3r_4 = g_{dd}(r_{13})l(k_F r_{12}), \quad (2.20)$$

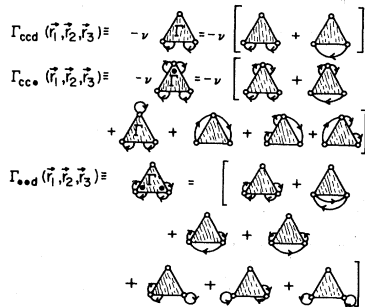


FIG. 6. Schematic graphical definitions of some three-body functions in terms of partial three-body functions of Fig. 5.

$$\Gamma_{ccd}(\vec{r}_1, \vec{r}_2, \vec{r}_3) = \hat{g}_{ccd}(\vec{r}_1, \vec{r}_2, \vec{r}_3) + l(k_f r_{12})g_{ddd}(\vec{r}_1, \vec{r}_2, \vec{r}_3) \quad (2.14)$$

and

$$\Gamma_{ccd}(\vec{r}_1, \vec{r}_2, \vec{r}_3) = g_{dd}(r_{13})\Gamma_{cc}(r_{12}) + Z_{cdc}(\vec{r}_1, \vec{r}_3; \vec{r}_2) - \frac{\rho}{\nu} \int Z_{cdc}(\vec{r}_1, \vec{r}_3; \vec{r}_4)\Gamma_{cc}(r_{42})d^3r_4, \quad (2.16)$$

where $Z_{cdc}(1,3;2)$ is non-nodal in point 2:

$$Z_{cdc}(\vec{r}_1, \vec{r}_3; \vec{r}_2) = \Gamma_{dd}(r_{23})\Gamma_{cc}(r_{12}) + Y_{dcc}(\vec{r}_3; \vec{r}_1, \vec{r}_2) - \frac{\rho}{\nu} \int Y_{dcc}(\vec{r}_3; \vec{r}_4, \vec{r}_2)\Gamma_{cc}(r_{41})d^3r_4, \quad (2.17)$$

where $Y_{dcc}(3;1,2)$ is non-nodal in both points 1 and 2; and

$$\frac{\rho}{\nu} \int Z_{cdc}(\vec{r}_4, \vec{r}_3; \vec{r}_2)l(k_F r_{41})d^3r_4 = \Gamma_{dd}(r_{23})l(k_F r_{12}), \quad (2.21)$$

$$\frac{\rho}{\nu} \int \Gamma_{cc\cdot}(\vec{r}_1, \vec{r}_4, \vec{r}_3)l(k_F r_{42})d^3r_4 = g_{d\cdot}(r_{13})l(k_F r_{12}) - \Gamma_{cc}(r_{13})l(k_F r_{32})/\nu. \quad (2.22)$$

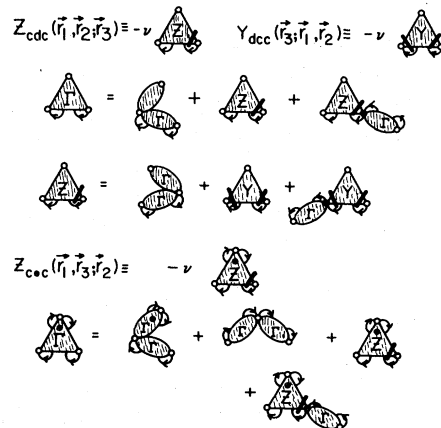


FIG. 7. Some partial three-body nodal equations, discussed in detail in the text.

III. KINETIC ENERGY

Various prescriptions have been discussed for the computation of the expectation value of the kinetic energy operator with respect to a correlated ground-state trial function [Eq. (1.1)].⁴ These prescriptions, being in principle equivalent to each other, are generated by integration by parts in the kinetic-energy expectation value. They may be transformed into one another by using the Jackson-Feenberg identity for a real correlation operator ψ_c (Ref. 1):

$$\psi_c \nabla^2 \psi_c = \frac{1}{2} (\nabla^2 \psi_c^2 + \psi_c^2 \nabla^2) + \frac{1}{2} \psi_c^2 [\nabla, [\nabla, \ln \psi_c]] - \frac{1}{4} [\nabla, [\nabla, \psi_c^2]]. \quad (3.1)$$

The most frequently used formulas for the variational kinetic energy derived by this procedure are the Clark-Westhaus (CW) form:

$$T_{\text{CW}} = T_F + I_0^{-1} \sum_i \frac{\hbar^2}{2m} \int |\nabla_i \psi_c|^2 |\Phi_0|^2 d\tau_1 \cdots d\tau_N \quad (3.2)$$

the Jackson-Feenberg (JF) form:

$$T_{\text{JF}} = T_F - \frac{1}{2} I_0^{-1} \sum_i \frac{\hbar^2}{2m} \int \{ |\Phi_0|^2 \nabla_i^2 \ln \psi_c - \frac{1}{2} \nabla_i^2 |\Phi_0|^2 \} \psi_c^2 d\tau_1 \cdots d\tau_N, \quad (3.3)$$

and the Iwamoto-Yamada or Pandharipande-Bethe form (PB):

$$T_{\text{PB}} = T_F - \frac{1}{2} I_0^{-1} \sum_i \frac{\hbar^2}{2m} \int [(\psi_c \nabla_i^2 \psi_c) |\Phi_0|^2 + \frac{1}{2} (\nabla_i \psi_c^2) \cdot \nabla_i |\Phi_0|^2] d\tau_1 \cdots d\tau_N, \quad (3.4)$$

where T_F is the free fermion kinetic energy

$$T_F = N \frac{3}{5} \frac{\hbar^2 k_f^2}{2m}.$$

These different forms of the kinetic-energy expectation value are, of course, identical as long as an exact (e.g., Monte Carlo) computation of the energy is performed. This is, however, in general no longer true if cluster expansion or integral equation approximations are used for their evaluation.

Nevertheless, each of the above-mentioned prescriptions has its specific advantages and disadvantages. This has been discussed amply in the literature; there is no need to reiterate the arguments here.

One of the main attractive features of the boson BGY equation is that the equivalence of these prescriptions for calculating the kinetic energy [obtained from Eqs. (3.2)–(3.4) by letting $\nu \rightarrow \infty$ at

fixed density] is maintained at each level of approximation.¹ We will see in Secs. IV and V that the fermion BGY equations maintain the equivalence between the CW and the PB forms,^{10,11} but some additional care must be exercised to retain the equivalence of the JF form to the other two. In the remainder of this section we formulate the expressions for the kinetic energy in terms of the two- and three-body functions defined in the last section.

We reiterate that we are concerned here with the case when the correlation operator is a Jastrow function [Eq. (1.2)]. In that case the terms in Eqs. (3.2)–(3.4) in which the gradient does not operate on the Slater determinant can be expressed simply in terms of the full two-body and three-body distribution functions, $g(r_{12})$ and $g_3(\vec{r}_1, \vec{r}_2, \vec{r}_3)$. The CW energy only has terms of this form, and can therefore be written as

$$T_{\text{CW}} = T_F + \frac{\hbar^2 \rho^2}{8m} \int d^3 r_1 \int d^3 r_2 g(r_{12}) \nabla_1 u(r_{12}) \cdot \nabla_1 u(r_{12}) + \frac{\hbar^2 \rho^3}{8m} \int d^3 r_1 \int d^3 r_2 \int d^3 r_3 g_3(\vec{r}_1, \vec{r}_2, \vec{r}_3) \nabla_1 u(r_{12}) \cdot \nabla_1 u(r_{13}). \quad (3.5)$$

(This will be the beginning point in Sec. IV for deriving T_{PB} and T_{JF} using the BGY equations.)

The last term in T_{JF} and in T_{PB} each involve a gradient of the square of the Slater determinant, and so will contain $\nabla_i l(k_F r_{ij})$. The operator is the

Laplacian in T_{JF} , producing reduced two-body terms proportional to $(\hbar^2/4m\nu^2)[\nabla_1 l(k_F r_{12})]^2$ and $(\hbar^2/4m\nu)\nabla_1^2 l(k_F r_{12})$ and a reduced three-body term proportional to $(\hbar^2/4m\nu^2)\nabla_1 l(k_F r_{12}) \cdot \nabla_1 l(k_F r_{13})$. To obtain a diagrammatic prescription for calculat-

ing the coefficients of these terms, we start with the generating function

$$G_0 = \ln I_0 ,$$

where I_0 is the normalization integral of the correlated trial function. G_0 is diagrammatically represented by the sum of all *biconnected* diagrams which can be constructed from the dynamical lines $h(r_{ij}) = e^{u(r_{ij})} - 1$ and the exchange lines $l(k_{fr_{ij}})/\nu$. The contribution of the differentiated exchange functions to the JF kinetic energy are then obtained by (1) replacing in turn each exchange line $l(k_{fr_{ij}})/\nu$ by $(\hbar^2/4m\nu)\nabla_i^2 l(k_{fr_{ij}})$, (2) replacing in turn each *connected pair* of exchange lines $l(k_{fr_{ij}})l(k_{fr_{ik}})/\nu^2$ by $(\hbar^2/4m\nu^2) \times \nabla_i l(k_{fr_{ij}}) \cdot \nabla_i l(k_{fr_{ik}})$, and (3) collecting all equivalent diagrams *after* steps (1) and (2). Clearly then, the coefficient of $[\nabla_1 l(k_{fr_{12}})]^2$ is a subset of the diagrams in $g_{dd}(r_{12})$, the coefficient of $\nabla_1^2 l(k_{fr_{12}})$ is a subset of $\Gamma_{cc}(r_{12})$, and the coefficient of $\nabla_1 l(k_{fr_{12}}) \cdot \nabla_1 l(k_{fr_{13}})$ is a subset of $\Gamma_{dcc}(\vec{r}_1, \vec{r}_2, \vec{r}_3)$. However, points \vec{r}_1 , \vec{r}_2 , and \vec{r}_3 are now effectively internal points, and therefore must

participate in the reduction to equivalent diagrams in step (3).

Equivalent diagrams are those diagrams which are not topologically equivalent until the convolution property of the statistical bonds, Eq. (2.1), is used to remove as many internal points as possible. Thus, the points \vec{r}_1 , \vec{r}_2 , and \vec{r}_3 must each be connected to at least one dynamical correlation line h . For example, the coefficient of $[\nabla_1 l]^2$ is $\Gamma_{dd}(r_{12})$, the term with no correlation lines between \vec{r}_1 and \vec{r}_2 having been eliminated. Moreover, as discussed in Sec. II, the convolution property of Γ_{cc} [Eq. (2.13)] together with the reduction rule has the consequence that c points which become internal points are not nodal points between Γ_{cc} and l . Thus the coefficient of $[\nabla_1 l(k_{fr_{12}})]^2$ is the non-nodal part of $\Gamma_{cc}(r_{12})$ namely $X_{cc}(r_{12})$ and the coefficient of $\nabla_1 l(k_{fr_{12}}) \cdot \nabla_1 l(k_{fr_{13}})$ is that part of $\Gamma_{dcc}(\vec{r}_1, \vec{r}_2, \vec{r}_3)$ which is non-nodal in points \vec{r}_2 and \vec{r}_3 and dynamically connected in point r_1 , which is the function $Y_{dcc}(\vec{r}_1, \vec{r}_2, \vec{r}_3)$ defined in Eq. (2.17) and Fig. 7. The total contribution of ∇l terms to the JF kinetic energy is shown in Fig. 8(a). Including the other terms in T_{JF} , the final result is

$$T_{JF} = T_F + \frac{\hbar^2 \rho^2}{8m} \int d^3 r_1 d^3 r_2 \left[-g(r_{12}) \nabla^2 u(r_{12}) - \frac{2}{\nu} \Gamma_{dd}(r_{12}) \nabla_1 l(k_{fr_{12}}) \cdot \nabla_1 l(k_{fr_{12}}) + 2X_{cc}(r_{12}) \nabla^2 l(k_{fr_{12}}) \right] \\ + \frac{\hbar^2 \rho^3}{4m} \int d^3 r_1 d^3 r_2 d^3 r_3 Y_{dcc}(\vec{r}_1, \vec{r}_2, \vec{r}_3) \nabla_1 l(k_{fr_{12}}) \cdot \nabla_1 l(k_{fr_{13}}) / \nu . \quad (3.6)$$

We emphasize that this is the most general form of the JF kinetic energy. Other forms have been given elsewhere which represent special approximations of the three-body function Y_{dcc} (e.g., superposition approximation, summation of "fan-like" diagrams, etc.).⁴⁶

A similar analysis is applicable to the last term of the PB kinetic-energy expression [Eq. (3.4)] which is proportional to $\nabla u \cdot \nabla l$ cross terms. The factor $\nabla_1 u(r_{12})$ provides a dynamical correlation

between points \vec{r}_1 and \vec{r}_2 , allowing for no further reduction to equivalent terms in those points. However, the third point in the three-body term is a c point and must be reduced. Thus, the coefficient of $\nabla_1 u(r_{12}) \cdot \nabla_1 l(k_{fr_{13}})$ is non-nodal in point three, which is the function $Z_{c-c}(\vec{r}_1, \vec{r}_2, \vec{r}_3)$ defined in Eq. (2.18) and Fig. 7 (which must be "rotated" so that the non-nodal point is \vec{r}_3). The ∇l term in the PB kinetic energy is shown in Fig. 8(b), giving the total PB kinetic energy as

$$T_{PB} = T_F - \frac{\hbar^2 \rho^2}{8m} \int d^3 r_1 d^3 r_2 \{ [2\nabla^2 u(r_{12}) + \nabla_1 u(r_{12}) \cdot \nabla_1 u(r_{12})] g(r_{12}) - 4\Gamma_{cc}(r_{12}) \nabla_1 u(r_{12}) \cdot \nabla_1 l(k_{fr_{12}}) / \nu \} \\ - \frac{\hbar^2 \rho^3}{8m} \int d^3 r_1 d^3 r_2 d^3 r_3 [g_3(\vec{r}_1, \vec{r}_2, \vec{r}_3) \nabla_1 u(r_{12}) \cdot \nabla_1 u(r_{13}) - 4Z_{c-c}(\vec{r}_1, \vec{r}_2, \vec{r}_3) \nabla_1 u(r_{12}) \cdot \nabla_1 l(k_{fr_{13}}) / \nu] . \quad (3.7)$$

IV. FERMION BGY EQUATIONS

The same type of analysis applied to the kinetic energy in the last section can be applied to the

derivation of the fermion BGY equation for $g(r_{12})$ [Eq. (1.16)]. Indeed, the generating function $G_0 = \ln I_0$ can be used to generate $g(r)$ by functional differentiation^{3,47}:

$$\frac{\hbar^2}{8m} \left\{ \text{diagram (a)} + 2 \left[\text{diagram (a)} + \text{diagram (a)} \right] \right\}$$

$$\frac{\hbar^2}{4m} \left\{ 2 \text{diagram (b)} \cdot \nabla_1 u_{12} + 2 \text{diagram (b)} \cdot \nabla_1 u_{12} \right\}$$

FIG. 8. $\vec{\nabla}l$ contributions to the JF kinetic-energy expression (a) and the PB kinetic-energy expression (b).

$$\frac{N\rho}{2} g(r) = \frac{\delta G_0}{\delta u(r)}. \quad (4.1)$$

Similarly, $\rho^2 g(r_{12})/2$ can be obtained as the coefficient of $V(r_{12})$ in the expectation value of the potential energy. Thus, $g(r_{12})$ is diagrammatically represented by replacing in turn each dynamical correlation $h(r_{ij})$ in G_0 by $e^{u(r_{ij})}$ and relabeling the points i and j as the external points 1 and 2. Consequently, all internal points in $g(r_{12})$ are biconnected and the two external points are at least singly connected to the remainder of the diagram. The diagrammatic expression for $\nabla_1 l(r_{12})$ is obtained from the diagrammatic expression for $g(r_{12})$ by (1) replacing in turn each dynamical correlation line connected to point 1 by $\nabla_1 h(r_{1i}) = \nabla_1 u(r_{1i}) e^{u(r_{1i})}$; (2) replacing in turn each exchange line connected to point 1, $l(k_F r_{1i})/\nu$ by $\nabla_1 l(k_F r_{1i})/\nu$, and (3) collecting all equivalent diagrams after steps 1 and 2. Note that r_1 and r_2 are external points and thus are not involved in the reduction to equivalent diagrams.

The point i which appears in steps 1 and 2 may be either the other external point \vec{r}_2 or one of the

$$\nabla_1 g(r_{12}) = g(r_{12}) \nabla_1 u(r_{12}) - 2\Gamma_{cc}(r_{12}) \nabla_1 l(r_{12})/\nu + \rho \int [g_3(\vec{r}_1, \vec{r}_2, \vec{r}_3) \nabla_1 u(r_{13}) - 2Z_{c-c}(\vec{r}_1, \vec{r}_2; \vec{r}_3) \nabla_1 l(k_F r_{13})/\nu] d^3 r_3. \quad (4.4)$$

Any method for solving this equation requires both Γ_{cc} and the two three-body functions g_3 and Z_{c-c} . These three-body functions can be expressed as functionals of the partial distribution functions defined in Sec. III, as will any useful approximation scheme. Thus, we are not only required to

$$2 \left[\text{diagram (a)} + \text{diagram (a)} \right]$$

FIG. 9. $\vec{\nabla}l$ terms in the FBGY equation for $\vec{\nabla}g(r_{12})$.

internal points which will be labeled \vec{r}_3 . It was pointed out in Sec. III that because of the exponential form of ψ_c , the terms multiplying $\vec{\nabla}_1 u(r_{12})$ add up to $g(r_{12})$ and the terms multiplying $\nabla_1 u(r_{13})$ add up to $g_3(\vec{r}_1, \vec{r}_2, \vec{r}_3)$. That this is consistent with step 1 above has to do with the fact that $\nabla_1 u(r_{1i}) e^{u(r_{1i})} = \nabla_1 u(r_{12}) [h(r_{1i}) + 1]$ so that diagrams which do not contribute to the $\nabla_1 u(r_{1i})$ term because the dynamic bond $h(r_{1i})$ is absent are exactly compensated by the term 1 in the bracket.

A similar compensation does *not* occur in the factor multiplying $\nabla_1 l(k_F r_{1i})$. Thus, it consists of all the diagrams which have an exchange connection between \vec{r}_1 and \vec{r}_i before collecting equivalent diagrams. In the case when $i=2$ so there is at least one direct exchange connection between \vec{r}_1 and \vec{r}_2 , the coefficient is just the dressed exchange bond $\Gamma_{cc}(r_{12})$. Thus, the two-body function in the BGY equations [Eq. (1.16)] is

$$\gamma(r_{12}) = -2\Gamma_{cc}(r_{12}), \quad (4.2)$$

where the factor of 2 is due to the two different directions of the exchange bond. Similarly, the coefficient of $\nabla_1 l(k_F r_{13})$ is the sum of all of the terms in $g_3(\vec{r}_1, \vec{r}_2, \vec{r}_3)$ which have at least one exchange path between \vec{r}_1 and \vec{r}_3 . However, since \vec{r}_3 is an internal point, equivalent terms must be collected at \vec{r}_3 . Thus, the three-body coefficient is non-nodal in point \vec{r}_3 , giving

$$\gamma_3(\vec{r}_1, \vec{r}_2; \vec{r}_3) = -Z_{c-c}(\vec{r}_1, \vec{r}_2; \vec{r}_3), \quad (4.3)$$

where Z_{c-c} is defined in Eq. (2.18) and Fig. 7. The two ∇l terms are shown diagrammatically in Fig. 9. The two-body FBGY equation is, then,

find an equation for Γ_{cc} , but also for all of the two-body partial distribution functions.

The expression of $g(r_{12})$ in terms of the partial distribution functions, Eq. (2.7) which we repeat here for convenience,

$$g(r_{12}) = [1 - l(k_F r_{12})^2/\nu] g_{dd}(r_{12}) + \Gamma_{de}(r_{12}) + \Gamma_{ed}(r_{12}) - 2l(k_F r_{12}) \hat{g}_{cc}(r_{12})/\nu + \hat{g}_{ee}(r_{12}), \quad (4.5)$$

has the advantage that all exchange correlations

directly between \vec{r}_1 and \vec{r}_2 are exhibited explicitly. Operating with $\vec{\nabla}_1$ does not change that fact. Indeed, collecting the $\nabla_1 l(k_f r_{12})$ terms provides a more direct demonstration of the result (4.2) for the coefficient of this factor. Moreover, the diagrammatic expressions for the $g_{\alpha\beta}(r_{12})$ (by which we mean g_{dd} , Γ_{de} , Γ_{ed} , \hat{g}_{ee} , and \hat{g}_{cc}) follow the same rules (stated above) for $g(r_{12})$ except that the

diagrams are restricted to those having the (α, β) exchange character of (\vec{r}_1, \vec{r}_2) . Consequently, the coefficient of $\nabla_1 u(r_{12})$ is just $g_{\alpha\beta}(r_{12})$ [which combine to give $g(r_{12})$ in the first term of Eq. (4.4)], there are no $\nabla_1 l(k_f r_{12})$ terms in $\nabla_1 g_{\alpha\beta}(r_{12})$ and the three-body terms must combine to give g_3 and $-2Z_{c.c.}$, respectively [using the weighting given the corresponding two-body term in Eq. (4.5)]. Thus,

$$\nabla_1 g_{\alpha\beta}(r_{12}) = g_{\alpha\beta}(r_{12}) \nabla_1 u(r_{12}) + \rho \int [g_{\alpha\beta\gamma}(\vec{r}_1, \vec{r}_2, \vec{r}_3) \nabla_1 u(r_{13}) + \gamma_{\alpha\beta\gamma}(\vec{r}_1, \vec{r}_2, \vec{r}_3) \nabla_1 l(k_f r_{13}) / \nu] d^3 r_3, \quad (4.6)$$

where

$$g_{\alpha\beta} = \{g_{dd}, \Gamma_{de}, \Gamma_{ed}, \hat{g}_{ee}, \text{ or } \hat{g}_{cc}\}.$$

In the two cases where $\alpha = d$ so that there is no exchange correlation between particle 1 and any other particle, the corresponding three-body function vanishes:

$$\gamma_{dd3} = \gamma_{de3} = 0. \quad (4.7)$$

In the dd equation, g_{dd3} is the sum of those terms in g_3 which have no exchange correlations at points 1 and 2:

$$g_{dd3}(\vec{r}_1, \vec{r}_2, \vec{r}_3) = g_{ddd}(\vec{r}_1, \vec{r}_2, \vec{r}_3) + g_{dde}(\vec{r}_1, \vec{r}_2, \vec{r}_3) \\ \equiv \Gamma_{dd}(\vec{r}_1, \vec{r}_2, \vec{r}_3). \quad (4.8)$$

Thus,

$$\vec{\nabla}_1 g_{dd}(r_{12}) = g_{dd}(r_{12}) \nabla_1 u(r_{12}) \\ + \rho \int [g_{ddd}(\vec{r}_1, \vec{r}_2, \vec{r}_3) + g_{dde}(\vec{r}_1, \vec{r}_2, \vec{r}_3)] \\ \times \nabla_1 u(r_{13}) d^3 r_3. \quad (4.9)$$

Except for the presence of g_{dde} on the right-hand side, this equation is quite similar to the boson BGY equation, Eq. (1.16). Moreover, $g_{dd}(r_{12})$ goes asymptotically to 1 and is positive, so that the

solution to this equation is quite similar to the boson $g(r)$. However, numerical experience shows that the fermion and the boson $g(r)$ are much more similar than $g_{dd}(r)$ and the boson $g(r)$. Exchange correlations, which appear both in g_{dde} and in internal bonds in g_{ddd} have a significant effect on g_{dd} as will be seen in the numerical solutions below.

The equation for $\Gamma(r_{12})$ has a similar structure. More compact expressions are obtained, however, if the equations are written for the functions $g_{d.}$, Γ_{cc} , and Γ_{ee} . The three-body factor in $\nabla_1 g_{d.}$ is the sum of all terms in g_3 in which point 1 is a d point, and point two is e, c , or d . (Point 2 can be a d point since $\nabla_1 g_{d.}$ contains $\nabla_1 g_{dd}$.) This sum of three-body terms is the auxiliary three-body function $\Gamma_{d.}(\vec{r}_1, \vec{r}_2, \vec{r}_3)$ defined similarly to the other auxiliary three-body functions in Fig. 6. Thus,

$$\nabla_1 g_{d.}(r_{12}) = g_{d.}(r_{12}) \nabla_1 u(r_{12}) \\ + \rho \int \Gamma_{d.}(\vec{r}_1, \vec{r}_2, \vec{r}_3) \nabla_1 u(r_{13}) d^3 r_3, \quad (4.10)$$

where

$$\Gamma_{d.}(\vec{r}_1, \vec{r}_2, \vec{r}_3) = \hat{g}_{dee}(\vec{r}_1, \vec{r}_2, \vec{r}_3) + g_{dde}(\vec{r}_1, \vec{r}_2, \vec{r}_3) + g_{ded}(\vec{r}_1, \vec{r}_2, \vec{r}_3) \\ - 2l(k_f r_{13}) \hat{g}_{dcc}(\vec{r}_1, \vec{r}_2, \vec{r}_3) + [1 - l^2(k_f r_{13}) / \nu] g_{ddd}(\vec{r}_1, \vec{r}_2, \vec{r}_3). \quad (4.11)$$

Clearly the coefficient of $\nabla_1 u(r_{13})$ in $\nabla_1 g_{d.}(r_{12})$ is the same auxiliary function but with points 1 and 2 interchanged; i.e., $\Gamma_{.d}(\vec{r}_1, \vec{r}_2, \vec{r}_3)$. There is also a $\nabla_1 l(k_f r_{13})$ term coming from those terms in $g_{.d}$ in which an exchange line goes directly from point 1 to point 3 and which are fully reduced in the internal point 3. Thus, the coefficient of $\nabla_1 l(k_f r_{13}) / \nu$

in the $.d$ equation is

$$\gamma_{.d3}(\vec{r}_1, \vec{r}_2, \vec{r}_3) = -2Z_{cdc}(\vec{r}_1, \vec{r}_2, \vec{r}_3), \quad (4.12)$$

where Z_{cdc} is defined in Eq. (2.16) and in Fig. 7 (note the permutation in coordinates) giving the ed FBGY equation

$$\begin{aligned} \nabla_1 g \cdot d(r_{12}) &= g \cdot d(r_{12}) \nabla_1 u(r_{12}) \\ &+ \rho \int [\Gamma \cdot d(\vec{r}_1, \vec{r}_2, \vec{r}_3) \nabla_1 u(r_{13}) - 2Z_{cdc}(\vec{r}_1, \vec{r}_2; \vec{r}_3) \nabla_1 l(k_F r_{13})] d^3 r_3 . \end{aligned} \quad (4.13)$$

Of course, in the uniform liquid $\nabla_1 g_d \cdot (r_{12}) = \nabla_1 g \cdot d(r_{12})$, so that (4.10) and (4.13) are equivalent. Thus, either of these equations or a linear combination can be used. The particular choice may be important when approximations are introduced and the equivalence is no longer automatic. We will comment on this further below.

By the same type of reasoning, the *cc* FBGY equation is

$$\begin{aligned} \nabla_1 \Gamma_{cc}(r_{12}) &= \Gamma_{cc}(r_{12}) \nabla_1 u(r_{12}) + g_{dd}(r_{12}) \nabla_1 l(k_F r_{12}) \\ &+ \rho \int [\Gamma_{cc}(\vec{r}_1, \vec{r}_2, \vec{r}_3) \nabla_1 u(r_{13}) - Z_{dcc}(\vec{r}_1, \vec{r}_2; \vec{r}_3) \nabla_1 l(k_F r_{13}) / \nu] d^3 r_3 , \end{aligned} \quad (4.14)$$

where $Z_{dcc}(\vec{r}_1, \vec{r}_2; \vec{r}_3) = Z_{cdc}(\vec{r}_2, \vec{r}_1; \vec{r}_3)$ is discussed above and Γ_{cc} is defined in Eq. (2.15) and Fig. 6.

A similar analysis produces the equation for $\nabla_1 \Gamma_{ee}$ though it is not necessary since, by Eq. (2.3),

$$\nabla_1 \Gamma_{ee}(r_{12}) = \nabla_1 g(r_{12}) - \nabla_1 \Gamma_{dd}(r_{12}) - \nabla_1 [\Gamma_{de}(r_{12}) + \Gamma_{ed}(r_{12})] , \quad (4.15)$$

giving

$$\begin{aligned} \nabla_1 \Gamma_{ee}(r_{12}) &= \Gamma_{ee}(r_{12}) \nabla_1 u(r_{12}) - 2\Gamma_{cc}(r_{12}) \nabla_1 l(k_F r_{12}) / \nu \\ &+ \rho \int \{ [g_3(\vec{r}_1, \vec{r}_2, \vec{r}_3) + \Gamma_{dd}(\vec{r}_1, \vec{r}_2, \vec{r}_3) - \Gamma_{d..}(\vec{r}_1, \vec{r}_2, \vec{r}_3) - \Gamma_{\cdot d}(\vec{r}_1, \vec{r}_2, \vec{r}_3)] \nabla_1 u(r_{13}) \\ &- 2[Z_{c \cdot c}(\vec{r}_1, \vec{r}_2, \vec{r}_3) - Z_{cdc}(\vec{r}_1, \vec{r}_2, \vec{r}_3)] \nabla_1 l(k_F r_{13}) / \nu \} d^3 r_3 . \end{aligned} \quad (4.16)$$

It should be emphasized that the diagrammatic analysis produces this result and not the equivalent result obtained by replacing Γ_{ed} by Γ_{de} (or vice versa) in Eq. (4.15). This suggests that any approximation scheme which sacrifices this equivalence should use as the equation for ∇g_d just one-half the sum of Eqs. (4.10) and (4.13).

We end this section by reexamining the equivalence of the Clark-Westhaus and Pandharipande-Bethe expressions for the kinetic energy, Eqs. (3.2) and (3.4), respectively. Beginning with the Clark-Westhaus result, we eliminate the $g_3 \nabla_1 u$ term by using the FBGY equation for ∇g [Eq. (4.4)], giving a fourth equation for the kinetic energy

$$\begin{aligned} \bar{T} &= T_F + \frac{\hbar^2 \rho^2}{8m} \int d^3 r_1 d^3 r_2 [-g(r_{12}) \nabla^2 u(r_{12}) + 2\Gamma_{cc}(r_{12}) \nabla_1 u(r_{12}) \cdot \nabla_1 l(k_F r_{12}) / \nu] \\ &+ \frac{\hbar^2 \rho^3}{4m} \int d^3 r_1 d^3 r_2 d^3 r_3 Z_{c \cdot c}(\vec{r}_1, \vec{r}_2, \vec{r}_3) \nabla_1 u(r_{12}) \cdot \nabla_1 l(k_F r_{13}) / \nu . \end{aligned} \quad (4.17)$$

(The fact that g_3 does not appear explicitly in this expression will prove useful in later discussions.)

Finally, T_{PB} is just a linear combination of T_{CW} and \bar{T} :

$$T_{PB} = 2\bar{T} - T_{CW} . \quad (4.18)$$

An important corollary to this result is that the equality of these three energies, $T_{PB} = T_{CW} = \bar{T}$ is preserved for any of the "natural" approximations in the FBGY method, by which we mean *approximations obtained by approximating the three-body functions in the FBGY equations*. The only requirement is that the same approximation for the three-body functions be used to compute the ener-

gies. Moreover, it is only the single FBGY equation for g which is required; i.e., the other independent two-body partial distribution functions may employ some other set of approximations (FHNC/*n*, for example).

The equivalence of the Jackson-Feenberg kinetic energy to these others does not follow in as a simple fashion from the FBGY equations, nor is it as easy to preserve within approximations (our earlier comments to the contrary notwithstanding^{10,11}) since as an additional quantity the non-nodal function $X_{cc}(r)$ is required. Since this function appears nowhere else in the analysis, we would be able to preserve the equivalence of the JF kinetic energy

by a suitable definition of X_{cc} but such a choice does not emerge in a natural way. The situation is clarified by a more detailed analysis of the cc equation in the next section.

V. THE cc EQUATION

The convolution property of $\Gamma_{cc}(r_{12})$ [Eq. (2.13)] which we rewrite as

$$\frac{\rho}{v} \int \Gamma_{cc}(r_{12}) l(k_F r_{20}) d^3 r_2 = l(k_F r_{10}), \quad (5.1)$$

played an essential role in our derivation of the

$$\begin{aligned} \nabla_1 \Gamma_{cc}(r_{12}) &= \Gamma_{cc}(r_{12}) \nabla_1 u(r_{12}) + g_{dd}(r_{12}) \nabla_1 l(k_F r_{12}) \\ &+ \rho \int d^3 r_3 \{ [-\Gamma_{cc}(r_{13}) \Gamma_{cc}(r_{23}) / v + Z_{c \cdot c}(\vec{r}_1, \vec{r}_3; \vec{r}_2)] \nabla_1 u(r_{13}) \\ &\quad - [\Gamma_{dd}(r_{13}) \Gamma_{cc}(r_{32}) + Y_{dcc}(\vec{r}_1; \vec{r}_2, \vec{r}_3)] \nabla_1 l(k_F r_{13}) / v \} \\ &- \frac{\rho^2}{v} \int d^3 r_3 d^3 r_4 [Z_{c \cdot c}(\vec{r}_1, \vec{r}_3; \vec{r}_2) \nabla_1 u(r_{13}) - v^{-1} Y_{dcc}(\vec{r}_1; \vec{r}_4 \vec{r}_3) \nabla_1 l(k_F r_{13})] \Gamma_{cc}(r_{42}), \end{aligned} \quad (5.3)$$

where the $g_{dd}(r_{13}) \Gamma_{cc}(r_{12}) \vec{\nabla} u(r_{13})$ has vanished due to the integration over \vec{r}_3 . This equation can be rearranged into the form

$$\vec{\nabla}_1 [\Gamma_{cc}(r_{12}) - l(k_F r_{12})] = \vec{\nabla}_1 P(r_{12}) - \frac{\rho}{v} \int \nabla_1 P(r_{13}) \Gamma_{cc}(r_{32}) d^3 r_3, \quad (5.4a)$$

where

$$\begin{aligned} \nabla_1 P(r_{12}) &\equiv \Gamma_{cc}(r_{12}) \nabla_1 u(r_{12}) + \Gamma_{dd}(r_{12}) \nabla_1 l(k_F r_{12}) \\ &+ \rho \int d^3 r_4 [Z_{c \cdot c}(1, 4; 2) \nabla_1 u(r_{14}) - Y_{dcc}(1; 2, 4) \nabla_1 l(k_F r_{14}) / v]. \end{aligned} \quad (5.4b)$$

Fourier transforming Eq. (5.4a) shows that any solution $\Gamma_{cc}(r_{12})$ of Eq. (5.3) satisfies the convolution property [Eq. (5.1)] provided that $\tilde{P}(k) \neq -v$. Moreover, it is seen that any approximate cc FBGY equation which is obtained from Eq. (5.3) by approximating the three-body functions Z_{cc} and Y_{dcc} maintains this convolution property.

Inspection of Eq. (5.3) reveals, however, the uncomfortable property that $\Gamma_{cc}(r_{12})$ obtained from an *arbitrary* (e.g., superposition approximation) choice of the three-body functions Z_{cc} and Y_{dcc} does not in general vanish for small r_{12} . This is caused by the fact that we have explicitly included the convolution integrals with Γ_{cc} [last terms in Eqs. (2.17) and (2.18)] in the definition of the three-body function, and miss thereby the factor of $g_{dd}(r_{12})$ which enforces the correct short-range

FBGY equations and the kinetic-energy expressions by reducing out all nodal contributions at internal c points. In momentum space this equation is

$$\Gamma_{cc}(k) = \tilde{l}(k), \quad k \leq k_F. \quad (5.2)$$

This convolution property is an exact property and thus is implicit in the cc FBGY equation. To make it explicit, we need to exhibit the nodal properties of $\Gamma_{cc}(\vec{r}_1, \vec{r}_2, \vec{r}_3)$ and $Z_{dcc}(\vec{r}_1 \vec{r}_2; \vec{r}_3)$ at point 2 which is accomplished by substituting Eq. (2.18) for Γ_{cc} and Eq. (2.17) (with $\vec{r}_1 \rightarrow \vec{r}_2$, $\vec{r}_3 \rightarrow \vec{r}_1$, $\vec{r}_2 \rightarrow \vec{r}_3$) for Z_{dcc} in the cc FBGY equation [Eq. (4.14)] giving

correlations. In order to obtain solutions of the cc equation which can be used for energy calculations with strongly repulsive interactions, we can pursue one of two alternatives:

(a) We can disregard the convolution property of $\Gamma_{cc}(r_{12})$ [Eq. (5.1)] and use approximations for Γ_{cc} and Z_{dcc} which have an explicit factor $g_{dd}(r_{12})$. This guarantees that $\Gamma_{cc}(r_{12})$ may be written in the form

$$\Gamma_{cc}(r_{12}) = g_{dd}(r_{12}) G_{cc}(r_{12}). \quad (5.5)$$

In our numerical investigations of liquid ${}^3\text{He}$ using the superposition approximation for Γ_{cc} and Z_{dcc} it turned out, however, that this choice was unfavorable in that the solutions we found converged only at densities below the equilibrium density, a result inferior to FHNC/0 and other approxima-

tions (see discussion in Sec. VII).

(b) We can use special forms for Z_{cc} and Y_{dcc} to guarantee both of the properties (5.1) and (5.5). Before carrying out this second alternative, we can illustrate the essence of the problem and the solution in a simpler case. The convolution property of Γ_{cc} is already present in the cc nodal equation [Eq. (2.12)] which we rewrite here.

$$\Gamma_{cc}(r_{12}) = l(k_f r_{12}) - \nu X_{cc}(r_{12}) + \rho \int X_{cc}(r_{13}) \Gamma_{cc}(r_{32}) d^3 r_3. \quad (5.6)$$

For example, this equation produces the result (5.1) [or equivalently, (5.2)]. However, just as Eq. (5.3) for $\nabla_1 \Gamma_{cc}$, this nodal equation conceals the fact that Γ_{cc} is proportional to g_{dd} [Eq. (5.5)]. The immediate conclusion is that X_{cc} must contain the terms $\Gamma_{dd}(r_{12})$ times the first and third term of (5.6), with the rest of X_{cc} proportional to g_{dd}

$$\begin{aligned} X_{cc}(r_{12}) = & g_{dd}(r_{12}) X_{cc}^0(r_{12}) \\ & - \nu^{-1} \Gamma_{dd}(r_{12}) \\ & \times \left[l(k_f r_{12}) + \rho \int X_{cc}(r_{13}) \Gamma_{cc}(r_{32}) d^3 r_3 \right]. \end{aligned} \quad (5.7)$$

Substituting this into (5.6) and collecting terms produces the equation for Γ_{cc} :

$$\begin{aligned} \Gamma_{cc}(r_{12}) = & g_{dd}(r_{12}) \left[-\nu X_{cc}^0(r_{12}) + l(k_f r_{12}) \right. \\ & \left. + \rho \int X_{cc}(r_{13}) \Gamma_{cc}(r_{32}) d^3 r_3 \right]. \end{aligned} \quad (5.8)$$

Clearly, the diagrammatic properties of X_{cc}^0 are those of the elementary cc diagrams. Indeed, comparing Eq. (5.8) to the FHNC equation for Γ_{cc} , we find that Eq. (5.8) is exactly the cc FHNC equation, with

$$X_{cc}^0(r_{12}) = E_{cc}(r_{12}). \quad (5.9)$$

Thus, in the context of the nodal equation, requiring both the convolution property and the correct short-range structure of Γ_{cc} to be maintained leads us to the cc FHNC equation. We now show that the same result holds when we begin with the cc FBGY equation. In the process we gain new insights into the Jackson-Feenberg kinetic energy.

We begin by analyzing Y_{dcc} and $Z_{c.c}$ in a manner similar to our treatment of X_{cc} in Eq. (5.7), thereby defining two new functions Y_{dcc}^0 and $Z_{c.c}^0$ (see Fig. 10):

$$\begin{aligned} Y_{dcc}(\vec{r}_1; \vec{r}_2, \vec{r}_3) = & g_{dd}(r_{12}) Y_{dcc}^0(\vec{r}_1; \vec{r}_2, \vec{r}_3) \\ & + \Gamma_{dd}(r_{12}) \left[\Gamma_{dd}(r_{13}) \Gamma_{cc}(r_{32}) - \frac{\rho}{\nu} \int Y_{dcc}(\vec{r}_1; \vec{r}_4, \vec{r}_3) \Gamma_{cc}(r_{42}) d^3 r_4 \right] \end{aligned} \quad (5.10)$$

and

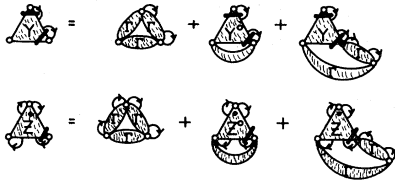
$$\begin{aligned} Z_{c.c}(\vec{r}_1, \vec{r}_3; \vec{r}_2) = & g_{dd}(r_{12}) Z_{c.c}^0(\vec{r}_1, \vec{r}_3; \vec{r}_2) \\ & - \Gamma_{dd}(r_{12}) \left[\Gamma_{cc}(r_{13}) \Gamma_{cc}(r_{32}) / \nu + \frac{\rho}{\nu} \int Z_{c.c}(\vec{r}_1, \vec{r}_3; \vec{r}_4) \Gamma_{cc}(r_{42}) d^3 r_4 \right]. \end{aligned} \quad (5.11)$$

Substituting these results into Eq. (5.3) produces an equation for $\nabla_1 \Gamma_{cc}$ which has a solution $\Gamma_{cc}(r_{12})$ which is manifestly proportional to $g_{dd}(r_{12})$ and satisfies the convolution relation:

$$\begin{aligned} \nabla_1 \Gamma_{cc}(r_{12}) = & \Gamma_{cc}(r_{12}) \nabla_1 u(r_{12}) + g_{dd}(r_{12}) \nabla_1 l(k_f r_{12}) \\ & + g_{dd}(r_{12}) \rho \int d^3 r_3 \{ [-\Gamma_{cc}(r_{13}) \Gamma_{cc}(r_{23}) / \nu + Z_{c.c}^0(\vec{r}_1, \vec{r}_2; \vec{r}_3)] \nabla_1 u(r_{13}) \\ & \quad - [\Gamma_{dd}(r_{13}) \Gamma_{cc}(r_{32}) + Y_{dcc}^0(\vec{r}_1; \vec{r}_2, \vec{r}_3)] \nabla_1 l(k_f r_{13}) / \nu \} \\ & - g_{dd}(r_{12}) \frac{\rho^2}{\nu} \int d^3 r_3 d^3 r_4 [Z_{c.c}(\vec{r}_1, \vec{r}_3; \vec{r}_4) \nabla_1 u(r_{13}) - Y_{dcc}(\vec{r}_1; \vec{r}_4, \vec{r}_3) \nabla_1 l(k_f r_{13}) / \nu] \Gamma_{cc}(r_{42}). \end{aligned} \quad (5.12)$$

Moreover, these two properties are satisfied for any approximations for the source terms $Z_{c.c}^0$ and Y_{dcc}^0 [which define the approximations for $Z_{c.c}$ and Y_{dcc}

through Eqs. (5.10) and (5.11), respectively]. One final piece of analysis demonstrates that Eq. (5.12) is in fact the gradient of the cc FHNC equation

FIG. 10. Fan diagram equations for Y_{dcc} and $Z_{c.c.}$.

[Eqs. (5.8) and (5.9)]. To motivate this we note that, while Y_{dcc}^0 is topologically elementary, $Z_{c.c.}^0$ still possesses parallel connections between points 1 and 2. These are illustrated in Fig. 11, which serves to define the elementary three-point function

FIG. 11. Schematic definition of the elementary three-point function $\xi_{c.c.}^0$.

$\xi_{c.c.}^0(\vec{r}_1, \vec{r}_3; \vec{r}_2)$. Substituting the equation of Fig. 11 into (5.12) and then using the definition of G_{cc} [Eq. (5.5)] in the first term of Eq. (5.12) and finally using the dd FBGY equation [Eq. (4.9)] to eliminate the resultant $G_{cc}g_{dd}\nabla_1 u$ and $G_{cc}\Gamma_{dd}\cdot\nabla_1 u$ terms, we obtain

$$\begin{aligned} \nabla_1 \Gamma_{cc}(r_{12}) = & G_{cc}(r_{12})\nabla_1 g_{dd}(r_{12}) + g_{dd}(r_{12})\nabla_1 l(k_f r_{12}) \\ & + g_{dd}(r_{12})\rho \int d^3 r_3 \{ [-\Gamma_{cc}(r_{13})\Gamma_{cc}(r_{32})/\nu + \xi_{c.c.}^0(\vec{r}_1, \vec{r}_3; \vec{r}_2)]\nabla_1 u(r_{13}) \\ & \quad - [\Gamma_{dd}(r_{13})\Gamma_{cc}(r_{32}) + Y_{dcc}^0(\vec{r}_1; \vec{r}_2, \vec{r}_3)]\nabla_1 l(k_f r_{13})/\nu \} \\ & - g_{dd}(r_{12})\frac{\rho^2}{\nu} \int d^3 r_3 d^3 r_4 [Z_{c.c.}(\vec{r}_1, \vec{r}_3; \vec{r}_4)\nabla_1 u(r_{13}) - Y_{dcc}(\vec{r}_1; \vec{r}_4, \vec{r}_3)\nabla_1 l(k_f r_{13})/\nu]\Gamma_{cc}(r_{42}). \end{aligned} \quad (5.13)$$

Finally, comparing this equation to the gradient of the cc FHNC equation [Eqs. (5.8) and (5.9)] we see that $\xi_{c.c.}^0(\vec{r}_1, \vec{r}_3; \vec{r}_2)$ and $Y_{dcc}^0(\vec{r}_1; \vec{r}_2, \vec{r}_3)$ are the sources of the FBGY equation for the elementary diagrams:

$$\nabla_1 E_{cc}(r_{12}) = -\frac{\rho}{\nu} \int [\xi_{c.c.}^0(\vec{r}_1, \vec{r}_3; \vec{r}_2)\nabla_1 u(r_{13}) - Y_{dcc}^0(\vec{r}_1; \vec{r}_2, \vec{r}_3)\nabla_1 l(k_f r_{13})/\nu] d^3 r_3, \quad (5.14)$$

while $Z_{c.c.}$ and Y_{dcc} are the sources of the FBGY equation for the non-nodal sum X_{cc} :

$$\begin{aligned} \nabla_1 X_{cc}(r_{12}) = & -\Gamma_{cc}(r_{12})\nabla_1 u(r_{12})/\nu - \Gamma_{dd}(r_{12})\nabla_1 l(k_f r_{12})/\nu \\ & - \frac{\rho}{\nu} \int [Z_{c.c.}(\vec{r}_1, \vec{r}_3; \vec{r}_2)\nabla_1 u(r_{13}) - Y_{dcc}(\vec{r}_1; \vec{r}_2, \vec{r}_3)\nabla_1 l(k_f r_{13})/\nu] d^3 r_3. \end{aligned} \quad (5.15)$$

[Notice that $X_{cc} = -P/\nu$ as defined in Eq. (5.4a).]

Concerning the kinetic energy, we may use this equation for $\nabla_1 X_{cc}$ to eliminate the two $\nabla_1 u \cdot \nabla_1 l$ terms in Eq. (4.17) for the kinetic energy, thereby producing the Jackson-Feenberg form in [Eq. (3.6)]. Consequently, we conclude that the JF kinetic energy is equal to the CW kinetic energy as long as Eq. (5.15) is satisfied for the approximate $Z_{c.c.}$ and Y_{dcc} . And we reiterate that the CW, PB, and \bar{T} energies are equivalent as long as the approximations for $Z_{c.c.}$, g_3 , and Γ_{cc} in these energies are also used to calculate $g(r_{12})$ through the FBGY equation (4.4).

VI. SUPERPOSITION APPROXIMATION

The FBGY equations for the two-body functions are coupled to three-body functions, which are coupled to four-body functions, etc. Tractable equations can be obtained only by somehow approximately closing this BGY hierarchy. A convenient method for accomplishing this at the two-body equation level parallels the method applied to boson-Jastrow functions. There it was pointed out by Abe and Stell that since the wave function is defined entirely in terms of a two-body function

$f(r_{12})=e^{u(r_{12})}$ it can be shown that the higher-order distribution functions g_n , $n > 2$ can be written as functionals of $g(r_{12})$.⁴⁴ The structure of this functional for g_3 in the boson system is

$$g_3(\vec{r}_1, \vec{r}_2, \vec{r}_3) = g(r_{12})g(r_{13})g(r_{31})e^{A(\vec{r}_1, \vec{r}_2, \vec{r}_3)}, \quad (6.1)$$

where A is a linked diagrammatic expansion in terms of renormalized bonds $\Gamma(r_{ij})=g(r_{ij})-1$.

In the case of a fermion-Jastrow function, a similar result holds for the partial distribution functions $\Gamma_{\alpha\beta\gamma}(\vec{r}_1, \vec{r}_2, \vec{r}_3)$ defined in Sec. II. We define functions $G_{\alpha\beta\gamma}$ by

$$\Gamma_{\alpha\beta\gamma}(\vec{r}_1, \vec{r}_2, \vec{r}_3) = g_{ddd}(\vec{r}_1, \vec{r}_2, \vec{r}_3)G_{\alpha\beta\gamma}(\vec{r}_1, \vec{r}_2, \vec{r}_3). \quad (6.2)$$

Then the Abe structure for g_{ddd} is

$$g_{ddd}(\vec{r}_1, \vec{r}_2, \vec{r}_3) = g_{dd}(r_{12})g_{dd}(r_{23})g_{dd}(r_{31}) \times e^{A_{ddd}(\vec{r}_1, \vec{r}_2, \vec{r}_3)} \quad (6.3)$$

where $A_{ddd}(\vec{r}_1, \vec{r}_2, \vec{r}_3)$ is a linked diagrammatic expansion in terms of the renormalized bonds $\Gamma_{\alpha\beta}$. The functions $G_{\alpha\beta\gamma}$ with $(\alpha\beta\gamma) \neq (ddd)$ are the sums of all linked $(\alpha\beta\gamma)$ diagrams which have no

$$\Gamma_{..d}(\vec{r}_1, \vec{r}_2, \vec{r}_3) \cong g_{ddd}(\vec{r}_1, \vec{r}_2, \vec{r}_3) [G_{ee}(r_{12}) + G_{de}(r_{32})G_{de}(r_{31}) + G_{de}(r_{32})G_{de}(r_{21}) + G_{de}(r_{12})G_{de}(r_{31}) + G_{de}(r_{21}) + G_{de}(r_{12}) + G_{de}(r_{31}) + G_{de}(r_{32}) + 1], \quad (6.7)$$

$$\Gamma_{cc.}(\vec{r}_1, \vec{r}_2, \vec{r}_3) \cong g_{ddd}(\vec{r}_1, \vec{r}_2, \vec{r}_3) [G_{cc}(r_{12})G_{cc.}(\vec{r}_1, \vec{r}_2, \vec{r}_3) - G_{cc}(r_{13})G_{cc}(r_{32})/\nu], \quad (6.8)$$

$$g_3(\vec{r}_1, \vec{r}_2, \vec{r}_3) \cong g_{ddd}(\vec{r}_1, \vec{r}_2, \vec{r}_3) \left[-1 + \frac{2}{\nu^2} G_{cc}(r_{12})G_{cc}(r_{23})G_{cc}(r_{31}) + 2G_{d.}(r_{12})G_{d.}(r_{23})G_{d.}(r_{31}) + \sum_{i < j}^3 \{ G_{de}(r_{ki})G_{de}(r_{kj}) + G_{ee}(r_{ij}) [G_{de}(r_{ik}) + G_{de}(r_{jk}) + 1] \} \right], \quad (6.9)$$

where $G_{d.} = G_{de} + 1$, $(i, j, k) = \text{perm}(1, 2, 3)$ and the superposition approximation for g_{ddd} is

$$g_{ddd}(\vec{r}_1, \vec{r}_2, \vec{r}_3) \cong g_{dd}(r_{12})g_{dd}(r_{23})g_{dd}(r_{31}). \quad (6.10)$$

This set of equations (5)–(10) defines the fermion generalization of the superposition approximation.

A similar analysis produces the superposition approximation for the three-body coefficients of $\nabla_{1l}(k_f r_{13})$ in the FBGY equations. The coefficient in the $\cdot d$ equation [Eq. (4.13)], $Z_{cdc}(\vec{r}_1, \vec{r}_2, \vec{r}_3)$ is equivalent to the coefficient in the cc equation (4.14) after a permutation of arguments: $Z_{cdc}(\vec{r}_2, \vec{r}_1, \vec{r}_3)$. This function is defined in Eq.

parallel connected ddd factors, the bonds which have at least one internal point being the renormalized bonds just mentioned and the bonds between external points being of the form $G_{\mu\nu}$ where

$$\Gamma_{\mu\nu} = g_{dd}G_{\mu\nu}. \quad (6.4)$$

The analysis which leads to the explicit equation for the $G_{\alpha\beta\gamma}$ is similar to the partial nodal analysis of the three-body functions given in Sec. II coupled with the results in Sec. V [Eqs. (5.10) and (5.11)], where the objective was to extract an explicit factor $g_{dd}(r_{12})$ from certain three-body functions. The result is that $G_{\alpha\beta\gamma}$ consists of three-body non-nodal terms and nodal terms which satisfy three-body nodal equations of the type derived in Sec. II. We defer the complete analysis since the approximations we will use here involve only the leading terms in these expressions. The approximations needed for the FBGY equations [Eqs. (4.8)–(4.16)] are

$$\Gamma_{ccd}(\vec{r}_1, \vec{r}_2, \vec{r}_3) \cong g_{ddd}(\vec{r}_1, \vec{r}_2, \vec{r}_3)G_{cc}(r_{12}), \quad (6.5)$$

$$\Gamma_{dd.}(\vec{r}_1, \vec{r}_2, \vec{r}_3) \cong g_{ddd}(\vec{r}_1, \vec{r}_2, \vec{r}_3) \times [G_{de}(r_{13}) + G_{ed}(r_{32}) + 1], \quad (6.6)$$

(2.16) and Fig. 7, from which it can be seen that the appropriate superposition approximation is

$$Z_{cdc}(\vec{r}_1, \vec{r}_2, \vec{r}_3) \cong g_{dd}(r_{12})\Gamma_{dd}(r_{23})\Gamma_{cc}(r_{31}). \quad (6.11)$$

The corresponding function in the ∇g equation

(4.4) is $Z_{c.c}(\vec{r}_1, \vec{r}_2, \vec{r}_3)$ which is defined in Eq. (3.18) and Fig. 7 and is approximated by

$$Z_{c.c}(\vec{r}_1, \vec{r}_2, \vec{r}_3) \cong \Gamma_{d.}(r_{12})\Gamma_{dd}(r_{23})\Gamma_{cc}(r_{31}) + g_{dd}(r_{12})\Gamma_{ed}(r_{23})\Gamma_{cc}(r_{31}) - \nu^{-1}\Gamma_{cc}(r_{12})\Gamma_{cc}(r_{23})\Gamma_{dd}(r_{31}). \quad (6.12)$$

The superposition approximation for the coefficient of $\nabla_1 l(k_f r_{13})$ in the ee equation (4.16) is obtained by replacing the $\Gamma_{d \cdot}(r_{12})$ by $\Gamma_{de}(r_{12})$ in this equation for $Z_{c \cdot c}$. The set of FBGY approximate equations obtained using these superposition ap-

proximations is simplified by first replacing the $\nabla_1 g_{dd}$ equation by $\nabla_1 \text{lng}_{dd}$ and then by using the dd equation to write the other equations for the ratios $G_{\alpha\beta}$. It is then straightforward algebra to find

$$\nabla_1 \text{lng}_{dd}(r_{12}) = \nabla_1 u(r_{12}) + \rho \int d^3 r_3 [g_{dd}(r_{23})g_{dd}(r_{31}) + g_{dd}(r_{23})\Gamma_{ed}(r_{31}) + g_{de}(r_{23})g_{dd}(r_{31})] \nabla_1 u(r_{13}), \quad (6.13)$$

$$\begin{aligned} \nabla_1 G_{de}(r_{12}) &= \nabla_1 G_{d \cdot}(r_{12}) \\ &= \rho \int d^2 r_3 [\Gamma_{ee}(r_{32})g_{dd}(r_{13}) + \Gamma_{de}(r_{32})\Gamma_{de}(r_{13}) + \Gamma_{de}(r_{32})g_{dd}(r_{13})] \nabla_1 u(r_{13}), \end{aligned} \quad (6.14)$$

$$\begin{aligned} \nabla_1 G_{ed}(r_{12}) &= \nabla_1 G_{\cdot d}(r_{12}) \\ &= \rho \int d^3 r_3 [g_{dd}(r_{23})\Gamma_{ee}(r_{31}) + \Gamma_{de}(r_{23})\Gamma_{ed}(r_{31}) + g_{dd}(r_{23})\Gamma_{ed}(r_{31})] \nabla_1 u(r_{13}) \\ &\quad - \frac{2\rho}{v} \int d^3 r_3 \Gamma_{dd}(r_{23})\Gamma_{cc}(r_{31}) \nabla_1 l(k_f r_{13}), \end{aligned} \quad (6.15)$$

$$\nabla_1 [G_{cc}(r_{12}) - l(k_f r_{12})] = -\frac{\rho}{v} \int d^3 r_3 [\Gamma_{cc}(r_{23})\Gamma_{cc}(r_{31}) \nabla_1 u(r_{13}) + \Gamma_{cc}(r_{23})\Gamma_{dd}(r_{31}) \nabla_1 l(k_f r_{13})], \quad (6.16)$$

$$\begin{aligned} \nabla_1 [G_{ee}(r_{12}) - G_{de}(r_{12})G_{ed}(r_{12}) + G_{cc}(r_{12})^2/v] \\ &= \rho \int d^3 r_3 [\Gamma_{ed}(r_{23})\Gamma_{ee}(r_{31}) + \Gamma_{ee}(r_{23})\Gamma_{de}(r_{31}) + \Gamma_{ed}(r_{32})\Gamma_{de}(r_{31})] \nabla_1 u(r_{13}) \\ &\quad - \frac{2\rho}{v} \int d^3 r_3 \Gamma_{ed}(r_{23})\Gamma_{cc}(r_{31}) \nabla_1 l(k_f r_{13}). \end{aligned} \quad (6.17)$$

The four expressions for the kinetic energy Eqs. (3.5)–(3.7) and (4.17) require some approximation for three-body distribution functions. The Clark-Westhaus form requires only $g_3(\vec{r}_1, \vec{r}_2, \vec{r}_3)$ which can be approximated by Eqs. (6.9)–(6.10). The Pandharipande-Bethe expression requires both g_3 and $Z_{c \cdot c}$ which can be approximated by Eq. (6.12). The Jackson-Feenberg expression requires

$Y_{dcc}(\vec{r}_1; \vec{r}_2, \vec{r}_3)$ which is defined in Eq. (2.17) and Fig. 7. The superposition approximation for this function is

$$Y_{dcc}(\vec{r}_1; \vec{r}_2, \vec{r}_3) \cong \Gamma_{dd}(r_{12})\Gamma_{dd}(r_{13})\Gamma_{cc}(r_{23}), \quad (6.18)$$

producing a simple expression for T_{JF} :

$$\begin{aligned} T_{JF} &\cong T_F + \frac{\hbar^2 \rho}{8m} \int d^3 r_1 d^3 r_2 [-g(r_{12})\nabla^2 u(r_{12}) - 2\Gamma_{dd}(r_{12})\nabla_1 l(k_f r_{12}) \cdot \nabla_1 l(k_f r_{12})/v + 2X_{cc}(r_{12})\nabla^2 l(k_f r_{12})] \\ &\quad + \frac{\hbar^2 \rho^2}{8m} \int d^3 r_1 d^3 r_2 d^3 r_3 \Gamma_{dd}(r_{12})\Gamma_{dd}(r_{13})\Gamma_{cc}(r_{23}) \nabla_1 l(k_f r_{12}) \cdot \nabla_1 l(k_f r_{13})/v. \end{aligned} \quad (6.19)$$

Finally, the superposition approximation for $Z_{c \cdot c}$ [Eq. (6.12)] can be used in Eq. (4.17) for \bar{T} , giving

$$\begin{aligned} \bar{T} &\cong T_F + \frac{\hbar^2 \rho^2}{8m} \int d^3 r_1 d^3 r_2 [-g(r_{12})\nabla^2 u(r_{12}) + 2\Gamma_{cc}(r_{12})\nabla_1 u(r_{12}) \cdot \nabla_1 l(k_f r_{12})/v] \\ &\quad + \frac{\hbar^2 \rho^3}{4m} \int d^3 r_1 d^3 r_2 d^3 r_3 [\Gamma_{d \cdot}(r_{12})\Gamma_{dd}(r_{23})\Gamma_{cc}(r_{31}) + g_{dd}(r_{12})\Gamma_{ed}(r_{23})\Gamma_{cc}(r_{31}) \\ &\quad - v^{-1}\Gamma_{cc}(r_{12})\Gamma_{cc}(r_{23})\Gamma_{dd}(r_{31})] \nabla_1 u(r_{12}) \cdot \nabla_1 l(k_f r_{13})/v. \end{aligned} \quad (6.20)$$

VII. RESULTS

The FBGY equations with the superposition approximation Eqs. (6.13)–(6.17), produced unsatis-

factory results when applied to liquid ^3He . While reasonable solutions were obtained for densities $\rho < 0.014 \text{ \AA}^{-3}$, we were able to show that there is no solution to the equations for larger densities.

Since the experimental equilibrium density is 0.0164 \AA^{-3} , this method is not useful for liquid ^3He .

The responsibility for the failure in this approximation is with the cc equation in the superposition approximation, Eq. (6.16). This equation can be solved algebraically in momentum space:

$$\tilde{G}_{cc}(k) = \frac{\tilde{l}(k) + \tilde{h}(k)\tilde{X}_{cc}(k)}{1 + \nu^{-1}\tilde{h}(k)}, \quad (7.1)$$

where the tilda indicates dimensionless Fourier transform, and $h(r)$ is defined by

$$\nabla h(r) = \Gamma_{cc}(r)\nabla u(r) + \Gamma_{dd}(r)\nabla l(k_f r).$$

On the other hand, the formal solution of the FHNC/0 equation for g_{cc} [Eq. (5.8) with $X_{cc}^0 \equiv E_{cc} = 0$] gives a similar equation

$$\tilde{G}_{cc}(k) = \frac{\tilde{l}(k) - \nu X_{cc}(k)^2}{1 - \tilde{X}_{cc}(k)}. \quad (7.2)$$

Although the only difference between (7.2) and (7.1) is the replacement of \tilde{h} by $-\nu\tilde{X}_{cc}$, that is a crucial difference since it turns out numerically that the denominator in (7.1) at $k = k_f$ approaches zero as the density increases to $\rho = 0.014 \text{ \AA}^{-3}$, while the denominator in (7.2) remains nonzero to much higher density. Moreover, using the fact that

$$\tilde{l}(k) = \nu, \quad k < k_f, \quad (7.3)$$

the FHNC/0 expression satisfies the exact result

$$\tilde{G}_{cc}(k) = \nu[1 + \tilde{X}_{cc}(k)], \quad k < k_f, \quad (7.4)$$

which is simply a restatement of the convolution property of $\Gamma_{cc}(r)$, i.e., is required by the Pauli principle.

Thus, we conclude that in order to apply the FBGY method to a quantum fluid at high density, it is essential to devise an approximation scheme which preserves the convolution property of Γ_{cc} at least to a very good approximation. Moreover, it was shown in Sec. V that choosing an approximation scheme which exactly preserves the Γ_{cc} convolution property is tantamount to using the FHNC equation for Γ_{cc} with some approximation for the elementary diagram function E_{cc} . Interpreting such an approximation as an approximation for the three-body functions Γ_{cc} and Z_{dcc} which appear in the FBGY equation [Eq. (4.14)] it was also shown in Sec. V that the JF expression for the kinetic energy will be equivalent to the other three (T_{CW} , T_{PB} , and \bar{T}) if the same approximation is

incorporated into the $g(r)$ FBGY equation [Eq. (4.4)], where Z_{dcc} appears as a term in $Z_{c\cdot c}$ and Γ_{cc} appears as a term in g_3 .

Instead of deducing this elementary diagram approximation for Γ_{cc} and Z_{dcc} we use here a hybrid approximation whereby the FHNC/0 approximation is used for Γ_{cc} but the superposition approximation is used for all three-body functions which appear in the FBGY equations for g and its components Γ_{dd} , Γ_{de} , and Γ_{ee} and also in the evaluation of kinetic energy. While this preserves the equivalence of the CW, PB, and \bar{T} kinetic energy, they will no longer be equivalent to the JF kinetic energy. The difference between these two energies can be used as one measure of the effect of this additional approximation.

The final step in our approximation scheme is motivated by the fact that the FBGY equations for $\Gamma_{d\cdot}$ and $\Gamma_{\cdot d}$ [Eqs. (6.14) and (6.15), respectively] do not have the same solution within the superposition approximation. Since these functions appear in $g(r)$ as the sum $\Gamma_{d\cdot} + \Gamma_{\cdot d}$, we replace the pair of equations (6.14) and (6.15) by the sum of the two, which is then interpreted as the equation for $2\Gamma_{d\cdot}$. We will designate this hybrid approximation by FBGY/SA//FHNC- cc /0.

To apply this theory to liquid ^3He , the Jastrow pseudopotential defining the wave function is taken to have the McMillan-Schiff-Verlet form^{13,15}

$$u(r) = - \left[\frac{b\sigma}{r} \right]^5, \quad (7.5)$$

where b is a variational parameter which we take to be the value obtained in the Monte Carlo variational calculation reported recently by Levesque.¹⁸ The parameter σ is the scale of the standard Lennard-Jones two-body potential, which is the interaction chosen in this calculation:

$$V(r) = 4\epsilon[(\sigma/r)^{12} - (\sigma/r)^6], \quad (7.6)$$

$$\epsilon = 10.22 \text{ K}, \quad \sigma = 2.556 \text{ \AA}.$$

The kinetic energy, potential energy, and energy per particle are given in Table I. Because of the hybridization of the approximation discussed above, there are two different kinetic energies: T_{JF} and the common value of \bar{T} , T_{CW} , and T_{PB} . The greatest numerical accuracy is obtained in T_{JF} , since the three-body terms contribute terms of order 10^{-3} K. Since the three-body term in \bar{T} [Eq. (4.17)] involves only one factor of ∇u , it is relatively small compared to the g_3 term in T_{CW} and T_{PB} , but it cannot be ignored.

TABLE I. Comparison of the energy per particle and its components in the present calculation (FBGY/SA//FHNC-cc/0) and the Monte Carlo results of Ref. 18.

ρ (\AA^{-3})	b	FBGY/SA//FHNC-cc/0					Monte Carlo		
		V/N (K)	T/N (K)	T_{JF}/N (K)	E/N (K)	E_{JF}/N (K)	V/N (K)	T/N (K)	E/N (K)
0.0076	1.10	-5.11	4.42	4.43	-0.68	-0.68			
0.0108	1.10	-7.78	6.63	6.64	-1.15	-1.14	-7.93	6.80	-1.14 ± 0.15
0.0120	1.12	-9.06	7.76	7.78	-1.30	-1.27	-9.27	8.02	-1.26 ± 0.15
0.0131	1.12	-10.06	8.66	8.69	-1.39	-1.37	-10.40	8.98	-1.42 ± 0.15
0.0141	1.12	-10.98	9.52	9.55	-1.46	-1.43	-11.27	9.95	-1.33 ± 0.15
0.0153	1.12	-12.07	10.58	10.62	-1.49	-1.45	-12.30	11.11	-1.20 ± 0.20
0.0164	1.12	-13.08	11.60	11.64	-1.48	-1.44	-13.27	12.37	-0.90 ± 0.20
0.0197	1.12	-16.05	14.86	14.92	-1.19	-1.13	-16.18	15.84	-0.34 ± 0.15

It can be seen from Table I that the difference between \bar{T} and T_{JF} is rather small, ranging from 0.01 K per particle to 0.06 K per particle in the density range of interest (the former figure is comparable to our numerical uncertainty).

A comparison of our results to Levesque's Monte Carlo calculation with the identical wave function shown in Fig. 12 and Table I demonstrates that the FBGY energy is quite accurate at low and intermediate densities, but falls too low at the higher densities of interest. It can be seen in Table I that most of the discrepancy between these results is due to the kinetic energy for which the two evaluations differ by up to 1 K at the highest density. The smaller differences in the potential energy are of the opposite sign, thus reducing the magnitude of the discrepancy in the energy.

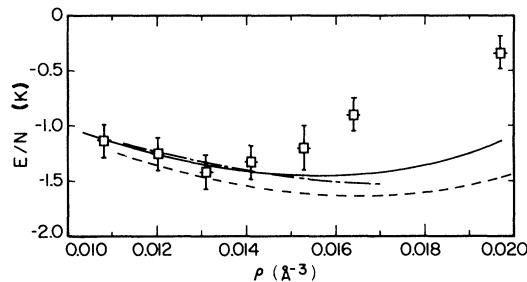


FIG. 12. Energy per particle for the fermion Jastrow function using the Schiff-Verlet-McMillan trial function [Eq. (7.5)] with the variational parameters determined in Ref. 18. The Monte Carlo results of Ref. 18 are the boxes with error bars. The solid line is the present calculation. The dashed line is the result of the boson-BGY plus Feenberg-Wu statistical approximation, Ref. 17. The dot-dash line is the FHNC/FBGY(dd) hybrid using the JF energy, Ref. 48.

The results of two other hybrid approximations have been reported elsewhere.⁴⁸ In that work the FBGY equation was used for g_{dd} but the FHNC equations were used for Γ_d , Γ_{ee} , and Γ_{cc} ; in one case the FHNC/0 approximation was used. The energy per particle for that FHNC/C//FBGY- dd /SA hybrid approximation using the JF kinetic energy is seen in Fig. 12 to be very close to the results obtained in the present work. Since the FBGY equation for ∇g is not satisfied in this hybrid, the several methods for evaluating the energy are not identical. Nevertheless, the discrepancy between the different evaluations of the energy is reduced substantially from the pure FHNC/0 and /C, e.g., at $\rho=0.014 \text{ \AA}^{-3}$, the difference between E_{CW} and E_{PB} is 0.75 K in the FHNC/C//FBGY- dd /SA approximation,⁴⁸ while it is 1.85 K in the FHNC/0 approximation,³⁸ 1.50 K in the FHNC/C approximation,⁴⁸ and 0.65 K in the FHNC/4 approximation.³⁸

Yet another approximation scheme can be compared to the present results. The earliest quantitatively successful many-body theory of the ground state of liquid ^3He was the statistical cluster expansion of Feenberg and Wu, where the energy and distribution functions of the trial fermion wave function of the form of (1.1) were expressed in terms of the boson distribution functions of ψ_c .¹ Schiff and Verlet used a Monte Carlo evaluation of these boson distribution functions together with the Feenberg-Wu expansion to obtain the energy of liquid ^3He in the wave functions that we have used in the present work.¹⁵ Further work in this regard was presented elsewhere, providing comparisons to the direct Monte Carlo evaluation of the energy in the fermion-Jastrow trial function.^{39,32} More in line with the philosophy of the present calculation,

several years ago Miller used the Feenberg-Wu method but with the boson $g(r)$ obtained by the boson HNC/0 and boson BGY/SA approximations.¹⁷ The energy obtained in the latter approximation is shown in Fig. 12 to be quite close to our present results.⁴⁹

Finally in Fig. 13 we show $g(r)$ and $g_{dd}(r)$ obtained from our FBGY/SA//FHNC-cc/0 calculation at $\rho=0.0142 \text{ \AA}^{-3}$ and $b=1.13$. These parameters are chosen to facilitate comparison with the Monte Carlo results for $g(r)$ obtained by Ceperley *et al.*³⁹ The difference between $g_{dd}(r)$ and $g(r)$ illustrates our earlier comments to the effect that $g_{dd}(r)$ is generally of the same character as $g(r)$ but somewhat less correlated. Comparison of the Monte Carlo to the FBGY $g(r)$ shows a disagreement very similar to the same comparison in a boson calculation.³⁶ The discrepancy near the maximum in $g(r)$ is larger than and in the opposite direction to the discrepancy between FHNC/0 and Monte Carlo, while the small r comparison favors FBGY. Moreover, a boson BGY calculation of $g(r)$ using the same approximations gives nearly identical results to the FBGY calculation, as is the case with Monte Carlo simulations.

VIII. DISCUSSION

In this paper we have presented a formal derivation of the generalization of the Born-Green-Yvon equations for the static distribution functions of a fermion-Jastrow description of the ground state of a fermion quantum fluid and a superposition approximation to truncate these equations. We have also derived analytic expressions for the Jackson-Feenberg and Pandharipande-Bethe forms of the kinetic energy expectation value and shown the role of the FBGY equations in establishing the

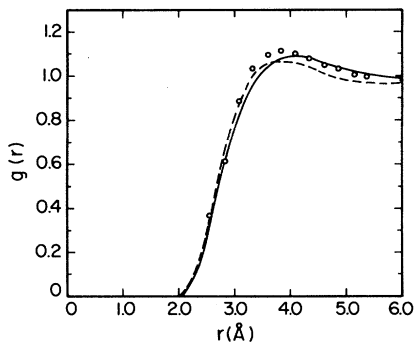


FIG. 13. $g(r)$ at $\rho=0.0142 \text{ \AA}^{-3}$ of the present calculation (solid line) and the Monte Carlo calculation of Ref. 39. The dashed line is $g_{dd}(r)$ in the present calculation.

equivalence of these energies and the Clark-Westhaus form.

An essential element in the present analysis is the Fermi-Cancellation property as manifested by the convolution property of the l function [Eq. (2.1)] and Γ_{cc} [Eq. (2.13)]. These convolution properties result in major cancellations between the partial distribution functions which appear in the FBGY equations and in the energies. Moreover, we found that when we ignored this property in our choice of approximation schemes we obtained unacceptable results. This led to the introduction of hybrid approximations which retain the Γ_{cc} convolution property by using an FHNC based approximation for Γ_{cc} .

The numerical results reported in the last section are reasonably good for the level of approximation. In particular, they are better than FHNC/0 and FHNC/C at low densities ($\rho \lesssim 0.014 \text{ \AA}^{-3}$), which suggests that this approximation scheme may be very useful in lower-density systems such as nuclear matter and spin-aligned deuterium.

The relationship of the FBGY/SA and FHNC/ n energies and the corresponding Monte-Carlo energies is the same as for boson systems, namely, for a given wave function, an FHNC/ n energy employing the JF form of the kinetic energy lies above the "exact" Monte Carlo evaluation while the FBGY/SA lies below.³⁶ This is not surprising since the major component of the fermion energy (ignoring the common free particle Fermi energy contribution T_F) is the boson part, and thus the largest part of the discrepancy is due to the errors in the boson part. Thus, the Miller calculation¹⁷ combining a boson BGY/SA approximation with a statistical cluster expansion agrees with the present results because the boson part of his approximation and ours is nearly equivalent.

An interesting feature of the FBGY method is that several different expressions of the kinetic energy— T_{CW} , T_{PB} , and \bar{T} —retain their equivalence for natural approximations, and the other commonly used expression, T_{JF} , is equivalent to the others if the convolution property of Γ_{cc} is maintained by the approximations. This has the advantage that one is not left with the question of which expression to use for the kinetic energy. However, this is also a disadvantage in that it removes the discrepancy between the kinetic energies as an internal measure of the accuracy of the approximation,³⁸ a significant drawback if there are no Monte Carlo results available for an external measure. It should be noted, however, that the

discrepancy between various forms of the kinetic energies is not a true measurement of the importance of the elementary diagrams. Our analysis shows that all forms of the kinetic energy can be transformed into one another using only planar diagrams. The discrepancy of the kinetic energies tells us only that some planar diagrams are omitted in the three-body distribution function. Thus, in Ref. 38, much of the improved self-consistency in going from FHNC/0 to FHNC/4 comes from improved approximations for the three-body functions.

Said another way, it is possible in principle to find approximations for the three-body distribution functions which produce the FHNC/ n approximation from the FBGY equations. Indeed, we showed exactly how to do this for the cc equation in Sec. V. If those same approximations are used in the kinetic-energy expressions, they will produce identical energies. Moreover, since the three-body terms contribute a negligible amount to the JF kinetic energy in liquid ${}^3\text{He}$ it follows that the common value of the kinetic energy when using consistent three-body approximations is just JF. Thus, to assess the effect of going from say FHNC/0 to FHNC/4 or FHNC/ C , one should compare the JF energies.

In regard to the differing values of the kinetic energy, it is worth noting that the form \bar{T} introduced in Eq. (4.17) may be a useful second choice of the energy in tandem with T_{JF} . Since T is the average of T_{CW} and T_{PB} , and in all calculations with which we are familiar T_{CW} is the largest and T_{PB} the smallest kinetic energy, then \bar{T} will be in closer agreement with T_{JF} than the other two. Moreover, since T_{JF} and \bar{T} are identical for boson systems, the discrepancy between \bar{T} and T_{JF} is a measure of the errors in the fermion contributions to the kinetic energy.

Finally, we can use the recent Monte Carlo calculations of Levesque to make an empirical decision about the best integral equation method for calculating the energy of liquid ${}^3\text{He}$. Comparing the results of Refs. 17, 38, 48, and the present calculations to the Monte Carlo results of Ref. 18, we find that the FHNC/4 approximation combined with the PB form for the kinetic energy falls within the Monte Carlo error bars for all densities calculated. Of the other calculations (all of which are of comparable difficulty to carry out numerically and considerably easier than the FHNC/4 approximation) the following fall within the Monte Carlo error bars for densities $\rho < 0.014 \text{ \AA}^{-3}$, but

fall below the Monte Carlo results at higher densities: the present results (FBGY/SA//FHNC- $cc/0$); FHNC/ α //FBGY- dd/SA , where α is 0 or C and the JF expression is used for the kinetic energy⁴⁸; and the boson BGY/SA plus Feenberg-Wu cluster expansion.¹⁷ In the density range $0.014 \text{ \AA}^{-3} < \rho < 0.017 \text{ \AA}^{-3}$, the following approximations are closest to the Monte Carlo results, lying above but near the error bars: FHNC/ α //FBGY- dd/SA where α is 0 or C and the CW expression for the kinetic energy⁴⁸; and the boson-HNC/0 approximation with the Feenberg-Wu cluster expansion.¹⁷ Evidently these approximations benefit from a partial cancellation of the errors of the boson part of the kinetic by the errors of the fermion part.

There are several directions in which the present work can be extended. Improvements upon the superposition approximation may be obtained by a generalization of the Abe-Stell expansion. Work on liquid ${}^4\text{He}$ (Ref. 36) suggests that the inclusion of higher-order terms in this expansion will produce significantly improved agreement with the exact result at higher densities.

To apply the present method to nuclear matter, it would be useful to include state dependence in the correlation function. As an alternative, one may also use the FBGY scheme to generate the compound diagrammatical quantities needed for the computation of off-diagonal matrix elements⁹ and single-particle energies.⁵⁰ These are the raw material for improving the variational estimates to the ground-state energy within the method of correlated basis functions.¹⁻⁶ They serve also for the computation of the quasiparticle interaction^{1,41,51} and BCS pairing matrix elements.⁵⁰

Finally, the one-body BGY equation has been successful in treating inhomogeneous classical fluids and boson quantum fluids, most notably in the difficult problem of the structure of the free surface of a fluid. We expect that the fermion one-body BGY equation will have similar usefulness in the theory of the surface of a fermion quantum fluid. Reference 52 contains a brief account of the work presented herein.

ACKNOWLEDGMENTS

This research was supported in part by National Science Foundation Grants No. DMR78-09226 and DMR-7926447, by the Deutsche Forschungsgemeinschaft and the U. S. Department of Energy, under Contract No. DE-AC02-76ER 13001. One of us (E.K.) would like to thank the Heisenberg foundation for financial support.

- *Present address: Institut für Theoretische Physik, Universität zu Köln, 5 Köln 41, W. Germany.
- ¹E. Feenberg, *Theory of Quantum Fluids* (Academic, New York, 1969).
 - ²C.-W. Woo, in *The Physics of Liquid and Solid Helium*, edited by K. H. Bennemann and J. B. Ketterson (Wiley, New York, 1976), Pt. 1, Chap. 5.
 - ³C. E. Campbell, *Progress in Liquid Physics*, edited by C. A. Croxton (Wiley, New York, 1978), Chap. 6; C. E. Campbell and F. J. Pinski, Nucl. Phys. A **328**, 210 (1979).
 - ⁴J. W. Clark in *Progress in Particle and Nuclear Physics*, edited by D. H. Wilkinson (Pergamon, Oxford, 1979), Vol. II.
 - ⁵B. D. Day, Rev. Mod. Phys. **50**, 495 (1978).
 - ⁶J. W. Clark, Nucl. Phys. A **328**, 587 (1979).
 - ⁷V. R. Pandharipande and R. B. Wiringa, Rev. Mod. Phys. **51**, 821 (1979).
 - ⁸S. Fantoni and S. Rosati, Nuovo Cimento A **25**, 593 (1975).
 - ⁹E. Krotscheck and M. L. Ristig, Nucl. Phys. A **242**, 389 (1975); E. Krotscheck, Phys. Lett. A **54**, 123 (1975); J. Low Temp. Phys. **27**, 199 (1977).
 - ¹⁰E. Krotscheck, Z. Phys. B **32**, 395 (1979).
 - ¹¹C. E. Campbell and K. E. Kürten (unpublished).
 - ¹²R. Jastrow, Phys. Rev. **98**, 1479 (1955).
 - ¹³W. L. McMillan, Phys. Rev. **138**, A442 (1965).
 - ¹⁴W. E. Massey, Phys. Rev. **151**, 153 (1966).
 - ¹⁵D. Schiff and L. Verlet, Phys. Rev. **160**, 208 (1967).
 - ¹⁶R. D. Murphy, Phys. Rev. A **5**, 331 (1972).
 - ¹⁷M. D. Miller, Phys. Rev. B **14**, 3937 (1976).
 - ¹⁸D. Levesque, Phys. Rev. B **21**, 5159 (1980).
 - ¹⁹C. E. Campbell and E. Feenberg, Phys. Rev. **188**, 396 (1969).
 - ²⁰C. C. Chang and C. E. Campbell, Phys. Rev. B **15**, 4238 (1977).
 - ²¹F. J. Pinski and C. E. Campbell, Phys. Lett. B **79**, 23 (1978).
 - ²²L. J. Lantto, A. D. Jackson, and P. J. Siemens, Phys. Lett. B **68**, 311 (1977).
 - ²³L. J. Lantto and P. J. Siemens, Phys. Lett. B **68**, 308 (1977); Nucl. Phys. A **317**, 55 (1979).
 - ²⁴J. C. Owen, Lect. Notes Phys. **142**, 280 (1981).
 - ²⁵E. Krotscheck, R. A. Smith, J. W. Clark, and R. M. Panoff (unpublished).
 - ²⁶V. R. Pandharipande and H. A. Bethe, Phys. Rev. C **7**, 1312 (1973).
 - ²⁷C.-W. Woo, Phys. Rev. Lett. **28**, 1442 (1972).
 - ²⁸C. E. Campbell, Phys. Lett. A **44**, 471 (1973).
 - ²⁹V. R. Pandharipande, Phys. Rev. B **18**, 218 (1978); K. E. Schmidt and V. R. Pandharipande, Phys. Rev. B **19**, 2504 (1979).
 - ³⁰K. Schmidt, M. H. Kalos, M. A. Lee, and G. V. Chester, Phys. Rev. Lett. **45**, 573 (1980).
 - ³¹S. Chakravarty and C.-W. Woo, Phys. Rev. B **13**, 4815 (1976); T. Li, E. Zhao, X. Zhu, and C.-W. Woo, Phys. Rev. B **21**, 2745 (1980).
 - ³²C. E. Campbell, T. C. Paulick, and L. R. Whitney, Nucl. Phys. A **317**, 135 (1979).
 - ³³J. M. J. van Leeuwen, J. Groeneveld, and J. de Boer, Physica (Utrecht) **25**, 792 (1959); T. Morita, Prog. Theor. Phys. **23**, 829 (1960).
 - ³⁴R. D. Murphy and R. O. Watts, J. Low Temp. Phys. **2**, 507 (1970).
 - ³⁵M. A. Pokrant, Phys. Rev. A **6**, 1588 (1972).
 - ³⁶R. A. Smith, A. Kallio, M. Puoskari, and P. Toropainen, Nucl. Phys. A **238**, 186 (1979).
 - ³⁷M. Gaudin, J. Gillespie, and G. Ripka, Nucl. Phys. A **176**, 237 (1971).
 - ³⁸J. Zabolitzky, Phys. Rev. A **16**, 1258 (1977).
 - ³⁹D. Ceperley, G. V. Chester, and M. H. Kalos, Phys. Rev. B **16**, 3081 (1977).
 - ⁴⁰E. Krotscheck, Nucl. Phys. A **317**, 149 (1979).
 - ⁴¹E. Krotscheck and R. A. Smith (unpublished).
 - ⁴²E. Krotscheck, Phys. Rev. A **15**, 397 (1977).
 - ⁴³M. Born and M. S. Green, *A General Kinetic Theory of Liquids* (Cambridge University, England, 1949); J. Yvon, *La Theorie Statistiques des Fluides et L'Equation D'Tat*, Actualities Scientifique et Industrielles (Hermann, Paris, 1935), Vol. 203.
 - ⁴⁴R. Abe, Prog. Theor. Phys. **21**, 421 (1959); G. Stell, Physica (Utrecht) **29**, 517 (1963).
 - ⁴⁵L. S. Ornstein and F. Zernike, Proc. Akad. Sci. (Amsterdam) **17**, 793 (1914).
 - ⁴⁶J. Dabrowski and W. Piechocki, Phys. Lett. B **84**, 20 (1979); S. Fantoni and S. Rosati, Phys. Lett. B **84**, 23 (1979).
 - ⁴⁷F. J. Pinski and C. E. Campbell, Chem. Phys. Lett. **56**, 156 (1978).
 - ⁴⁸E. Krotscheck, Z. Phys. B **32**, 395 (1979).
 - ⁴⁹A small part of the discrepancy between the present results and Miller's in Fig. 12 is due to the slightly different optimum value of b obtained by Miller.
 - ⁵⁰E. Krotscheck and J. W. Clark, Nucl. Phys. A **333**, 77 (1980).
 - ⁵¹H. T. Tan and E. Feenberg, Phys. Rev. **176**, 360 (1968).
 - ⁵²C. E. Campbell, K. E. Kürten, and E. Krotscheck, Lect. Notes Phys. **142**, 328 (1981).